ANALYSIS AND SIMULATION
OF MULTIRATE SAMPLED-DATA SYSTEMS

Anthony P. Messuri

Submitted in Partial Fulfillment of the Requirements

for the Degree of

Master of Science in Engineering

in the

Electrical Engineering

Program

Robert H. Foulkes, Jr. 6-1-79

Adviser Date

Leon Rand 6-11-79

Dean of the Graduate School Date

YOUNGSTOWN STATE UNIVERSITY

June, 1979

ABSTRACT

ANALYSIS AND SIMULATION

OF MULTIRATE SAMPLED-DATA SYSTEMS

Anthony P. Messuri

Master of Science in Engineering

Youngstown State University, 1979

This thesis deals with the analysis and simulation modeling of several multirate sampled-data system configurations. The analysis of these systems first requires the development of the discrete-time system description and finding the optimal feedback control matrix for such a system. An observer was included in the system representation to produce an approximation to the state vector, which is usually not available for direct measurement. Specific examples of multirate systems, having several different configurations were investigated. Computer simulation results are presented as well as a comparison of the responses of each system.

ACKNOWLEDGEMENTS

I would like to express my gratitude to Dr. Robert H. Foulkes Jr. for his interest and guidance on this project. I would also like to thank my family for their patience with me during this period, and especially my brother Dominic whose encouragement and enthusiasm contributed largely to the completion of this thesis.

TABLE OF CONTENTS

PAGE

LIST OF FIGURES

CHAPTER I

INTRODUCTION

Sampled-data analysis has been greatly motivated by the wide-spread use of digital computers in the implementation of feedback control systems. The formal study of sampled-data systems may be traced back to the development of automatic tracking radar systems during World War II. The pulsing characteristics of the radar position data led the designers to model the system as a sampled-data system rather than a continuous system. Interestingly, one of the main applications of sampled-data systems today is in the use of on-board microcomputers for guidance and control of aircraft systems. Since some of these guidance measurements may be monitored more slowly than others while still meeting the system performance requirements, more than one sampling rate may be present in the control system. These multirate sampled-data control systems result in a reduction in the amount of computer capacity and allow more system flexibility.

In this thesis, examples of multirate sampled-data systems are investigated. A development of the system equations describing a sampled-data control system is presented in detail in Chapter II. Also presented is the solution of this discrete-time optimization problem.

Chapter III includes a discussion of discrete-time systems in which the control variables are sampled at more than one rate. This leads to a simulation model representing a multirate sampled-data system.

Some specific examples of sampled-data control systems are considered in Chapter IV. A digital simulation was performed for each system and the resulting system response of each model is presented.

CHAPTER II

THE DISCRETE-TIME LINEAR QUADRATIC OPTIMIZATION PROBLEM

A. Development of the Discrete-Time System Description

The continuous-time equations describing a linear time-invariant control system are given by

$$\dot{x}(t)=Ax(t)+Bu(t) \tag{2.1}$$

$$y(t)=Cx(t) \tag{2.2}$$

where $x(t)$ denotes the state vector

$u(t)$ denotes the input vector

$y(t)$ denotes the output vector

and A, B, and C represent time-invariant coefficient matrices. In addition, the performance criteria for such a control system is given by the standard quadratic cost functional:

$$J=\int_{t_c}^{t_f}\left[x'(t)Qx(t)+u'(t)Ru(t)\right]dt \tag{2.3}$$

where Q and R are weighting matrices to be chosen by the designer (see [1,3-5]).

Matrix Q is selected to be symmetric and at least positive semidefinite while matrix R is selected to be symmetric and positive definite. In most cases, Q and R are chosen to be diagonal so that each individual component of the vectors $x(t)$ and $u(t)$ can be weighted separately. It can be seen from equation (2.3) that the larger the values of the matrix Q are chosen to be, the more rapidly $x(t)$ will converge to zero. Similarly, the larger the values of R, the more rapidly u(t) will converge to zero [6].

The set of equations (2.1), (2.2), and (2.3) is referred to as a linear quadratic optimization problem. The optimal solution consists of finding the input vector u(t) which satisfies the system equations (2.1) and (2.2) while minimizing the quadratic cost functional (2.3).

If a digital simulation of the sampled-data system described by equations (2.1) and (2.2) is to be implemented and tested on a computer, then their equivalent discrete-time deterministic equations must be obtained. This transformation to an equivalent discrete-time problem can be accomplished by integrating the differential equation (2.1) of the system and also the quadratic cost functional equation (2.3) over each sampling period [7].

Rewriting equation (2.1)

$$\dot{x}(t)=Ax(t)+Bu(t) \tag{2.4}$$

Applying the properties of Laplace Transforms produces

$$sIX(s)-X(0)=AX(s)+BU(s)$$

$$sIX(s)-AX(s)=X(0)+BU(s)$$

$$(sI-A)X(s)=X(0)+BU(s)$$

$$X(s)=(sI-A)^{-1}X(0)+(sI-A)^{-1}BU(s)$$

$$x(t)=e^{At}x(t_0)+\mathcal{L}^{-1}\left\{(sI-A)^{-1}BU(s)\right\} \tag{2.5}$$

Use of the convolution theorem [8]

$$\mathcal{L}^{-1}\left\{G(s)H(s)\right\}=(g*h)(t)$$

$$\mathcal{L}^{-1}\left\{G(s)H(s)\right\}=\int_{t_0}^{t}g(\alpha)h(t-\alpha)d\alpha \tag{2.6}$$

so in this case

$$\mathcal{L}^{-1}\left\{(sI-A)^{-1}BU(s)\right\}=e^{At}*Bu(t)$$

$$\mathcal{L}^{-1}\left\{(sI-A)^{-1}BU(s)\right\}=\int_{t_o}^{t}e^{A(t-\alpha)}Bu(\alpha)d\alpha \tag{2.7}$$

Substituting this result into equation (2.5) produces

$$x(t)=e^{At}x(t_o)+\int_{t_o}^{t}e^{A(t-\alpha)}Bu(\alpha)d\alpha \tag{2.8}$$

Since the functions involved in equation (2.8) are constant over definite intervals and sampling occurs only at the sampling instant t_k, the interval of integration may be changed from $[t_0, t]$ to $[t_k, t_{k+1}]$ yielding

$$x(t_{k+1})=e^{A(t_{k+1}-t_k)}x(t_k)+\int_{t_k}^{t_{k+1}}e^{A(t_{k+1}-\alpha)}Bu(\alpha)d\alpha \tag{2.9}$$

Assuming that u(t) is constant over the sampling period t_k, as mentioned above, also means that

$$u(t)=u(t_k) \qquad \text{for } [t_k, t_{k+1}] \tag{2.10}$$

and equation (2.9) can be rewritten as

$$x(t_{k+1})=e^{A(t_{k+1}-t_k)}x(t_k)+\left[\int_{t_k}^{t_{k+1}}e^{A(t_{k+1}-\alpha)}d\alpha\right]Bu(t_k) \tag{2.11}$$

which can be put in the form

$$x_{k+1}=\emptyset(t_{k+1},t_k)x_k+\int_{t_k}^{t_{k+1}}\emptyset(t_{k+1},s)dsBu_k \tag{2.12}$$

where $x_k=x(t_k)$

$u_k=u(t_k)$

$\emptyset(t_{k+1},t_k)=e^{A(t_{k+1}-t_k)}$

Further simplification of equation (2.12) yields

$$x_{k+1}=\emptyset x_k+Tu_k \tag{2.13}$$

where $\emptyset=\emptyset(t_{k+1},t_k)=e^{A(t_{k+1}-t_k)}$

$T=T(t_{k+1},t_k)=\int_{t_k}^{t_{k+1}}\emptyset(t_{k+1},s)dsB$

The discrete-time equivalent of equation (2.2) may be found directly from the continuous-time equation

$$y(t)=Cx(t)$$

Since the output measurement vector is sampled at discrete points in time, the discrete-time equivalent equation can be written as

$$y(t_k)=Cx(t_k) \tag{2.14}$$

or equivalently, since

$$y_k=y(t_k) \quad \text{and} \quad x_k=x(t_k)$$

then equation (2.14) may be rewritten as

$$y_k=Cx_k \tag{2.15}$$

In order to find a discrete-time equivalent of the quadratic cost functional equation (2.3), it must be rewritten as a sum of N integrals in much the same fashion as was done to form equation (2.12) of the discrete-time linear differential equation (2.4). The discrete-time cost functional equation then becomes [7]

$$J_N=\tfrac{1}{2}\left\{\sum_{k=0}^{N}(x'_{k+1}\hat{Q}x_{k+1}+2x'_k\hat{M}u_k+u'_k\hat{R}u_k)\right\} \tag{2.16}$$

where $\hat{Q}=\int_{t_k}^{t_{k+1}}\emptyset'(t,t_k)Q\emptyset(t,t_k)dt$

$\hat{M}=\int_{t_k}^{t_{k+1}}\emptyset'(t,t_k)QT(t,t_k)dt$

$\hat{R}=\int_{t_k}^{t_{k+1}}[R+T'(t,t_k)QT(t,t_k)]dt$

In summary, the linear quadratic optimization problem for the discrete-time case is given by the following set of equations:

$$x_{k+1}=\emptyset x_k+Tu_k \tag{2.17}$$

$$y_k=Cx_k \tag{2.18}$$

$$J_N=\tfrac{1}{2}\left\{\sum_{k=0}^{N}(x'_{k+1}\hat{Q}x_{k+1}+2x'_k\hat{M}u_k+u'_k\hat{R}u_k)\right\} \tag{2.19}$$

B. Solution of the Discrete-Time Linear Quadratic Optimization Problem

The solution of the system described by equations (2.17), (2.18), and (2.19) depends on determining the optimum value of the control input u_k which will minimize the quadratic cost functional J_N. One approach to the solution of this problem involves applying the principle of optimality to the quadratic cost function [9].

Beginning with the last term of the summation in equation (2.19)

$$J_N=\tfrac{1}{2}(x'_{N+1}\hat{Q}x_{N+1}+2x'_N\hat{M}u_N+u'_N\hat{R}u_N) \tag{2.20}$$

Substituting for the terms x_{k+1} as given by equation (2.17) yields

$$J_N=\tfrac{1}{2}[(\emptyset x_N+Tu_N)'\hat{Q}(\emptyset x_N+Tu_N)+2x'_N\hat{M}u_N+u'_N\hat{R}u_N] \tag{2.21}$$

Applying the following properties of matrices

$$(A+B)'=A'+B' \quad \text{and} \quad (AB)'=B'A' \tag{2.22}$$

equation (2.21) can be rewritten

$$J_N=\tfrac{1}{2}[x'_N\emptyset'\hat{Q}\emptyset x_N+x'_N\emptyset'\hat{Q}Tu_N+u'_NT'\hat{Q}\emptyset x_N+u'_NT'\hat{Q}Tu_N+$$
$$2x'_N\hat{M}u_N+u'_N\hat{R}u_N] \tag{2.23}$$

Since $\hat{Q}$ is symmetric

$$x'_N\emptyset'\hat{Q}Tu_N+u'_NT'\hat{Q}\emptyset x_N=2x'_N\emptyset'\hat{Q}Tu_N$$

Also, by factorization,

$$2x'_N\emptyset'\hat{Q}Tu_N+2x'_N\hat{M}u_N=2x'_N(\emptyset'\hat{Q}T+\hat{M})u_N$$

$$u'_NT'\hat{Q}Tu_N+u'_N\hat{R}u_N=u'_N(T'\hat{Q}T+\hat{R})u_N$$

Then equation (2.23) becomes

$$J_N=\tfrac{1}{2}[(x'_N\emptyset'\hat{Q}\emptyset x_N)+(2x'_N(\emptyset'\hat{Q}T+\hat{M})u_N)+u'_N(T'\hat{Q}T+\hat{R})u_N] \tag{2.24}$$

In order to minimize J_N, equation (2.24) will be differentiated with respect to u_N. It should be noted that x_N depends only on u_{N-1} and is not affected by u_N; therefore $\frac{\partial x_N}{\partial u_N}=0$. Applying the following properties, where B is symmetric

$$\frac{\partial}{\partial A}[A'BA]=2[BA] \quad \text{and} \quad \frac{\partial}{\partial A}[BA]=B'$$

Recalling that the matricies $\hat{Q}$ and $\hat{R}$ are symmetric, the derivative of J_N with respect to u_N is

$$\frac{\partial J_N}{\partial u_N}=0=\tfrac{1}{2}\left\{[0]+[2x'_N(\phi'\hat{Q}T+\hat{M})]'+[2(T'\hat{Q}T+\hat{R})u_N]\right\}$$

$$0=\tfrac{1}{2}[2(\phi'\hat{Q}T+\hat{M})'x_N]+[2(T'\hat{Q}T+\hat{R})u_N]$$

$$0=[(T'\hat{Q}\phi+\hat{M}')x_N]+[(T'\hat{Q}T+\hat{R})u_N]$$

Solving for u_N

$$u_N=-(T'\hat{Q}T+\hat{R})^{-1}(T'\hat{Q}\phi+\hat{M}')x_N \tag{2.25}$$

Equation (2.25) can be rewritten in the form

$$u_N=-H_Nx_N \tag{2.26}$$

where $$H_N=(T'\hat{Q}T+\hat{R})^{-1}(T'\hat{Q}\phi+\hat{M}') \tag{2.27}$$

Equation (2.26) represents the optimum value of the control input u_N which will minimize the N^{th} term of the cost functional J_N. Evaluating the cost functional equation (2.24) by substituting the value of u_N as given by equation (2.26) yields

$$J_N=\tfrac{1}{2}[(x'_N\phi'\hat{Q}\phi x_N)+(2x'_N(\phi'\hat{Q}T+\hat{M})(-H_Nx_N)+$$
$$(-(H_N)x_N)'(T'\hat{Q}T+\hat{R})(-H_Nx_N)]$$

$$J_N=\tfrac{1}{2}\left\{x'_N[(\phi'\hat{Q}\phi)+2(\phi'\hat{Q}T+\hat{M})(-H_N)+(-H'_N)(T'\hat{Q}T+\hat{R})(-H_N)]x_N\right\}$$

Substituting the value of H_N found in equation (2.27) produces

$$J_N=\tfrac{1}{2}\left\{x'_N[(\phi'\hat{Q}\phi)-2(\phi'\hat{Q}T+\hat{M})H_N+(T'\hat{Q}\phi+\hat{M}')'((T'\hat{Q}T+\hat{R})')^{-1}\right.$$
$$\left.(T'\hat{Q}T+\hat{R})(H_N)]x_N\right\}$$

$$J_N=\tfrac{1}{2}\left\{x'_N[(\phi'\hat{Q}\phi)-(\phi'\hat{Q}T+\hat{M})H_N]x_N\right\} \tag{2.28}$$

Equation (2.28) now represents the minimum value of the N^{th} term of the cost functional.

Using a similar approach, the $(N-1)^{th}$ term has the form

$$J_{N-1}=\tfrac{1}{2}(x'_N\hat{Q}x_N+2x'_{N-1}\hat{M}u_{N-1}+u'_{N-1}\hat{R}u_{N-1})+J_N$$

$$J_{N-1}=\tfrac{1}{2}(x'_N\hat{Q}x_N+2x'_{N-1}\hat{M}u_{N-1}+u'_{N-1}\hat{R}u_{N-1})+$$
$$\tfrac{1}{2}\left\{x'_N[(\phi'\hat{Q}\phi)-(\phi'\hat{Q}T+\hat{M})H_N]x_N\right\}$$

$$J_{N-1}=\tfrac{1}{2}\left(x'_N\left\{\hat{Q}+\left[(\emptyset'\hat{Q}\emptyset)-(\emptyset'\hat{Q}T+\hat{M})H_N\right]\right\}x_N+2x'_{N-1}\hat{M}u_{N-1}+\right.$$
$$\left.u'_{N-1}\hat{R}u_{N-1}\right) \tag{2.29}$$

Letting $P_{N-1}=\hat{Q}+\left[(\emptyset'\hat{Q}\emptyset)-(\emptyset'\hat{Q}T+\hat{M})H_N\right]$ (2.30)

allows equation (2.29)to be rewritten as

$$J_{N-1}=\tfrac{1}{2}(x'_N P_{N-1}x_N+2x'_{N-1}\hat{M}u_{N-1}+u'_{N-1}\hat{R}u_{N-1}) \tag{2.31}$$

Using equation (2.27) as the definition of the H_N term in equation (2.30), the matrix P_{N-1} is seen to be symmetric. Then equation (2.31) is equivalent to equation (2.20) with the index N replaced by N-1 and with P_N defined to be $\hat{Q}$. Therefore the optimum value of the control input u_{N-1} which will minimize the $(N-1)^{th}$ term of the cost functional J_{N-1} is

$$u_{N-1}=-H_{N-1}x_{N-1} \tag{2.32}$$

where $H_{N-1}=(T'P_{N-1}T+\hat{R})^{-1}(T'\hat{Q}\emptyset+\hat{M}')$

Note that equation (2.32) is equivalent to equation (2.26) with the index N replaced by N-1. According to Dorato and Levis [10], if the system is stable and controllable then the sequence P is bounded, and the discrete Riccati equation

$$P_{k-1}=\hat{Q}+\left[(\emptyset'P_k\emptyset)-(\emptyset'P_kT+\hat{M})H_k\right] \quad , \quad P_N=\hat{Q}$$

has a limiting solution P that satisfies

$$P=\hat{Q}+\left[(\emptyset'P\emptyset)-(\emptyset'PT+\hat{M})(T'PT+\hat{R})^{-1}(T'P\emptyset+\hat{M}')\right]$$

Therefore the optimum control input equation is

$$u_K=-Hx_K \tag{2.33}$$

where $H=(T'PT+\hat{R})^{-1}(T'P\emptyset+\hat{M}')$ (2.34)

and $P=\hat{Q}+\left[(\emptyset'P\emptyset)-(\emptyset'PT+\hat{M})H\right]$

The matrix H described by equation (2.34) represents the optimal feedback control matrix for the system given by equations (2.17), (2.18), and (2.19). The configuration of this system may be represented in block diagram form as shown in Figure 1.

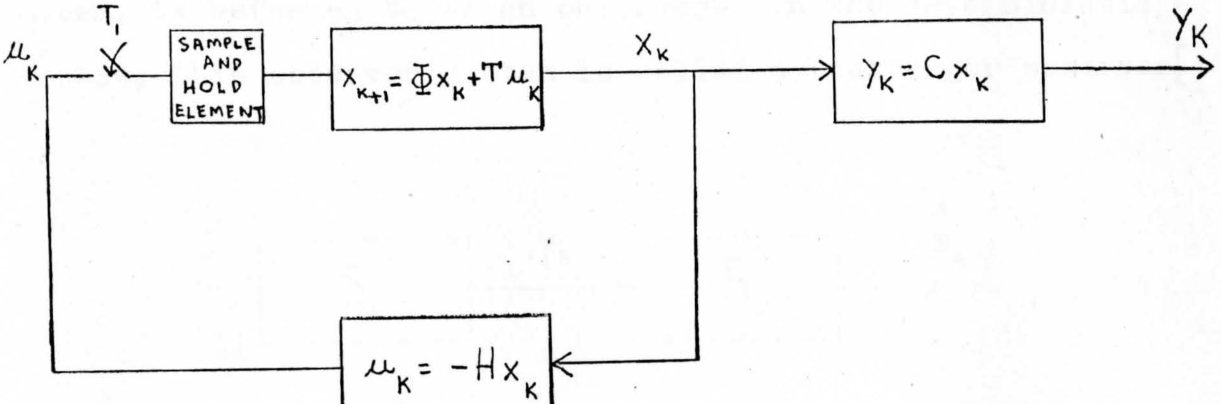

Figure 1. System Representation With Optimal Feedback Control Matrix.

C. Approximation of the State Vector

The system represented in Figure 1 requires that the entire state vector x(t) be directly available for use by the feedback controller. In an actual system, the entire state vector is usually not available for direct measurement. This requires the development of an approximate state vector which can then be substituted into the control law of equation (2.33). The system which produces an approximation of the state vector, using the inputs u_k and outputs y_k of the system, is referred to as an observer. In the deterministic case, this observer system is called a Luenberger observer[11].

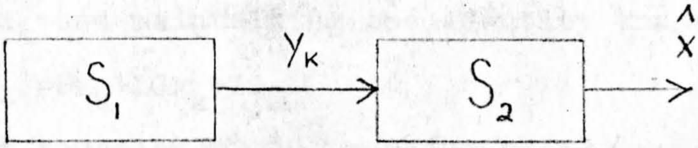

Figure 2. A Simple Observer System.

First, consider a system of the form of Figure 2, which shows a free system S_1 with no input and an observer S_2 whose inputs are the outputs of S_1. The equation describing system S_1 is

$$x_{k+1}=\emptyset x_k \quad , \quad y_k=Cx_k \tag{2.35}$$

and the equation describing the observer S_2 is

$$\hat{x}_{k+1}=F\hat{x}_k+Ly_k \tag{2.36}$$

The design of a Luenberger observer depends upon the existence of a transformation matrix V which satisfies the equation

$$V\emptyset-FV=LC \tag{2.37}$$

For convenience, the transformation matrix V may be chosen to be an identity transformation. When this is done V=I and equation (2.37) becomes

$$\emptyset-F=LC \tag{2.38}$$

Solving equation (2.38) for F yields

$$F=\emptyset-LC \tag{2.39}$$

Substituting equation (2.39) into equation (2.36)

$$\hat{x}_{k+1}=(\emptyset-LC)\hat{x}_k+Lx_k \tag{2.40}$$

Extending this principle to the forced system shown in Figure 3 will lead to an observer that can be described by an equation

$$\hat{x}_{k+1}=F\hat{x}_k+Ly_k+VTu_k \tag{2.41}$$

Since $y_k=Cx_k$ and maintaining the identity transformation V=I

$$\hat{x}_{k+1}=F\hat{x}_k+LCx_k+Tu_k \tag{2.42}$$

Noting that equation (2.39) remains valid

$$\hat{x}_{k+1}=(\emptyset-LC)\hat{x}_k+LCx_k+Tu_k \tag{2.43}$$

Any matrix L may be chosen for the observer; however the response of the observer system is determined by the eigenvalues of the matrix ($\emptyset$-LC). It should be noted that the response of the system decays exponentially for eigenvalues within the unit circle in the z-plane. The eigenvalues of the observer are chosen to be within the unit circle to insure system stability and that the state of the observer will converge to the state of the observed system. In practice, the eigenvalues of the observer are chosen to be slightly closer to the origin than the system eigenvalues to insure that the response of the observer will decay faster than the system response. Two different methods which were used to obtain observer matrices are presented in Appendix B.

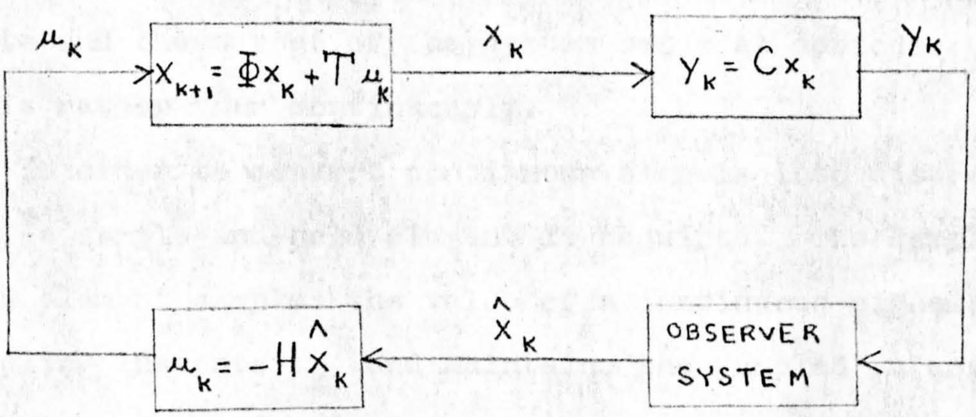

Figure 3. General Representation of a Feedback Control System With an Observer.

CHAPTER III

MODELING OF A MULTIRATE SAMPLED-DATA SYSTEM

A. Sampler Operation

The control system discussed thus far is referred to as a sampled-data system, since the system variables are only measured at discrete instants of time. Therefore samples of the state and the output of the system occur at periodic intervals rather than continuously.

In order to convert continuous signals into discrete signals, a sample-and-hold element is required. The sample-and-hold element samples the value of a continuous signal at the sampling instants t_k, and maintains the sampled value until the next sampling instant t_{k+1}. That is,

$$w(t)=w(t_k) \quad \text{for} \quad t_k \leq t < t_{k+1}$$

where $w(t)$ is the output of the sample-and-hold element. This description allows information to be converted from a continuous signal to a discrete signal and, likewise, from discrete to continuous. This operation is necessary in any design involving a digital computer since the computer cannot work with continuous signals directly. Instead, a digital computer performs its operations on distinct numbers available only at specific instants of time. In some applications, sample-and-hold elements are used because the sampling action may improve the overall performance of the system.

B. Multirate Sampling

Sampled-data systems may contain more than one sample-and-hold element. Most control systems are designed with the samplers operating in synchronism with the same sampling rate, and are thus referred to as single-rate sampled-data systems. However there exists a class of control systems in which two or more samplers operate with different sampling rates; these systems are referred to as multirate sampled-data systems. The analysis and design of multirate systems may be traced directly to problems concerned with single-rate sampled-data systems. That is, the designer may wish to convert a single-rate sampled system into a multirate system in order to analyze the system mathematically. Furthermore, the introduction of multirate sampling may be used to improve system response.

On the other hand, multirate sampling may arise from the modeling of an actual physical system. For instance, an onboard digital computer used in an aircraft flight control system may operate at a different rate than that of the various sensor inputs, such as the system radar (see [2,12-14]).

C. Representation of a Multirate System

The principle of multirate sampling can be applied to the discrete-time system described by the previously derived system equations

$$x_{k_M+1}=\emptyset x_{k_M}+Tu_{k_M}$$

$$y_{k_1}=Cx_{k_M}, \qquad k_M T_M=k_1 T_1$$

$$u_{k_M}=u_{k_2}, \qquad k_2 T_2 \leq k_M T_M < k_2 T_2+T_2$$

$$u_{k_2}=-H\hat{x}_{k_M}, \qquad k_2 T_2=k_M T_M$$

$$x_{k_M+1}=(\emptyset-LC)\hat{x}_{k_M}+Ly_{k_1}+Tu_{k_M}, \qquad k_1 T_1 \leq k_M T_M < k_1 T_1+T_1$$

which are represented by the system block diagram of Figure 4 containing two samplers. The two samplers shown operate at different sampling rates although both are assumed to close simultaneously at time t=0. The sampling rates T_1 and T_2 are assumed not to be integer multiples of each other. Therefore the smallest periodic interval for the entire multirate system is given by the least common multiple of T_1 and T_2, which will be denoted as T_M.

D. Sampling and Updating of System Variables

From Figure 4, it can be seen that u_{k_2} must be available at the sampling instants T_2. For this reason, the feedback control gain matrix H is calculated at T_2. Also, since x(t) and $\hat{x}_{k_M}$ must be available at both T_1 and T_2, these terms will be updated at the multiple time T_M.

Since y_{k_1} is only updated at T_1, the observer only receives new inputs at time T_1. Keeping this fact in mind, equation (2.43)

$$\hat{x}_{k_M+1}=(\emptyset-LC)\hat{x}_{k_M}+LCx_{k_M}+Tu_{k_2}$$

can be rewritten as

$$\hat{x}_{k_M+1}=(\emptyset-LC)\hat{x}_{k_M}+Ly_{k_1}+Tu_{k_2}$$

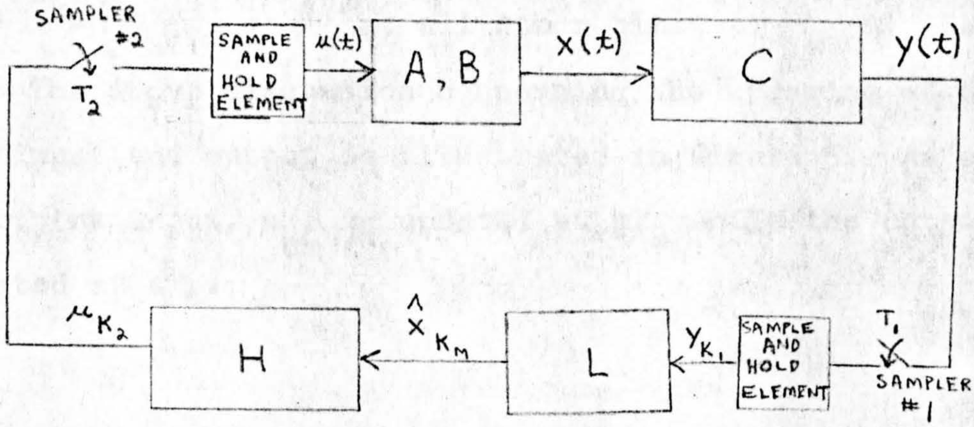

Figure 4. Multirate System Representation With T_1 Not Equal to T_2.

$$\hat{x}_{k_M+1}=\phi\hat{x}_{k_M}+Tu_{k_M}+L(y_{k_1}-C\hat{x}_{k_M}) \tag{3.1}$$

In order to update $\hat{x}_{k_M}$ at the multiple time T_M, a linear estimator can be used to calculate $\hat{x}_{k_M}$ at times other than T_1. According to Rhodes [15], the best linear estimator may be obtained by setting the observer term L equal to zero at all the times other than T_1. This approach results in the following observer description:

$$\hat{x}_{k_M+1}=\phi\hat{x}_{k_M}+Tu_{k_M}+z_{k_M}$$

where $$z_{k_M}=\begin{cases} L(y_{k_1}-C\hat{x}_{k_M}) & \text{at } k_MT_M=k_1T_1 \\ 0 & \text{at all other times} \end{cases} \tag{3.2}$$

The above discussion concerning the updating of the system input and output is illustrated in Figure 5. As can be seen, the input, u_{k_2}, is updated at k_2T_2 while the output, y_{k_1}, is updated at k_1T_1.

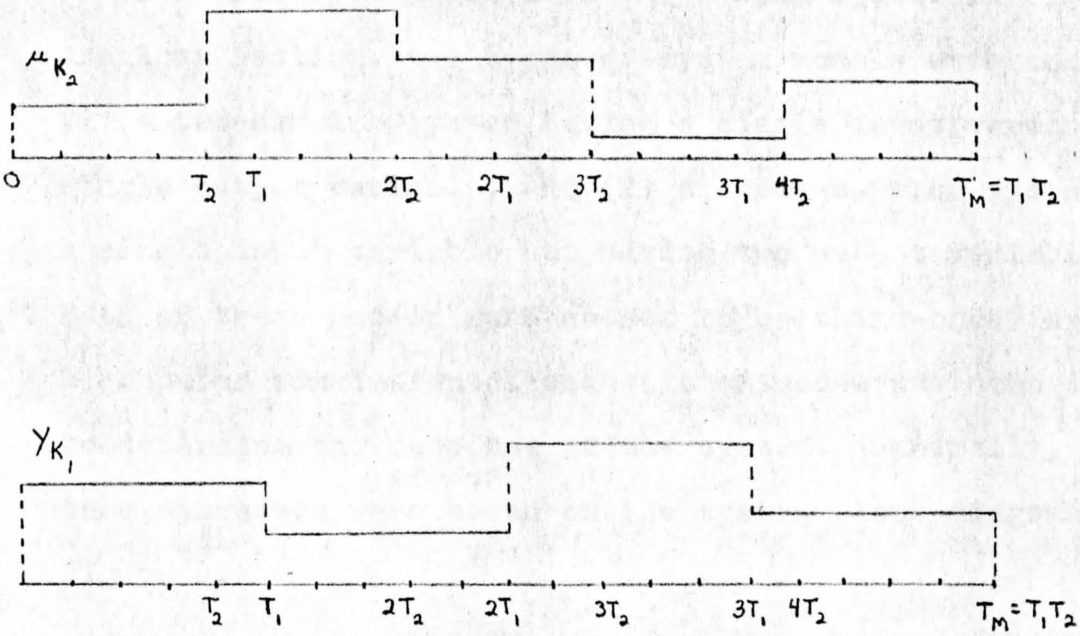

Figure 5. Sampling and Updating of System Variables

CHAPTER IV

EXAMPLES OF SPECIFIC MULTIRATE SYSTEMS

In order to demonstrate the implementation of a sampled-data system based on the system equations of the previous section, two types of system models were considered: (1) a two-sampler system having a single input variable and a single output variable; and (2) a three-sampler system having a single input variable but having two output variables. Both of these models were chosen to be third-order systems. A computer simulation of each system model was done in order to determine the response of the system. Generally, the systems discussed were based on the system block diagram shown in Figure 4.

A. Systems With Two Samplers

Consider the continuous-time system described by the following equations:

$$\begin{bmatrix} \dot{x}_1(t) \\ \dot{x}_2(t) \\ \dot{x}_3(t) \end{bmatrix} = \begin{bmatrix} -0.5 & 0.5 & 0.0 \\ -2.0 & -0.5 & 0.0 \\ 1.0 & 2.0 & 0.0 \end{bmatrix} \begin{bmatrix} x_1(t) \\ x_2(t) \\ x_3(t) \end{bmatrix} + \begin{bmatrix} 2.0 \\ 3.0 \\ 1.0 \end{bmatrix} \begin{bmatrix} u(t) \end{bmatrix}$$

$$\begin{bmatrix} y(t) \end{bmatrix} = \begin{bmatrix} 1.0 & 4.0 & 2.0 \end{bmatrix} \begin{bmatrix} x_1(t) \\ x_2(t) \\ x_3(t) \end{bmatrix}$$

$$J_0=\int_{t_o}^{T}\left\{\begin{bmatrix}x_1(t) & x_2(t) & x_3(t)\end{bmatrix}\begin{bmatrix}10.0 & 0.0 & 0.0\\ 0.0 & 10.0 & 0.0\\ 0.0 & 0.0 & 20.0\end{bmatrix}\begin{bmatrix}x_1(t)\\ x_2(t)\\ x_3(t)\end{bmatrix}+\begin{bmatrix}u(t)\end{bmatrix}\begin{bmatrix}2.0\end{bmatrix}\begin{bmatrix}u(t)\end{bmatrix}\right\}dt$$

where the A matrix was formed as shown in Appendix A. As discussed previously, the weighting matricies Q (t) and R (t) were chosen to be diagonal, and the values of these matricies were chosen by experimentation.

The particular two-sampler system chosen was one with a configuration as shown in Figure 4, sampler one operates at a rate of 4 samples per second while the rate of sampler two is 5 samples per second. In a multirate system, the smallest periodic interval, T_M, is given by the least common multiple of the two sampling intervals. Therefore for this particular system, the multiple sampling rate is 20 samples per second.

As discussed previously, the matricies Ø and T were computed at the multiple sampling rate while the gain matrix H was computed at the rate of sampler two. The discrete-time equations

$$x_{k_M+1}=\emptyset x_{k_M}+Tu_{k_M} \qquad u_{k_2}=-H\hat{x}_{k_M}$$

$$\hat{x}_{k_M+1}=\emptyset\hat{x}_{k_M}+Tu_{k_M}+L(y_{k_1}-C\hat{x}_{k_M}) \qquad y_{k_1}=Cx_{k_M}$$

become
$$\begin{bmatrix}x_1(k_M+1)\\ x_2(k_M+1)\\ x_3(k_M+1)\end{bmatrix}=\begin{bmatrix}0.9741 & 0.0244 & 0.0\\ -0.0975 & 0.9741 & 0.0\\ 0.0444 & 0.1 & 1.0\end{bmatrix}\begin{bmatrix}x_1(k_M)\\ x_2(k_M)\\ x_3(k_M)\end{bmatrix}+\begin{bmatrix}0.1006\\ 0.1432\\ 0.0598\end{bmatrix}\begin{bmatrix}u(k_M)\end{bmatrix}$$

$$\begin{bmatrix}y(k_1)\end{bmatrix}=\begin{bmatrix}1.0 & 4.0 & 2.0\end{bmatrix}\begin{bmatrix}x_1(k_M)\\ x_2(k_M)\\ x_3(k_M)\end{bmatrix}$$

$$\begin{bmatrix} u(k_2) \end{bmatrix} = -\begin{bmatrix} 7.0271 & -2.4795 & -1.3092 \end{bmatrix} \begin{bmatrix} \hat{x}_1(k_M) \\ \hat{x}_2(k_M) \\ \hat{x}_3(k_M) \end{bmatrix}$$

$$\begin{bmatrix} \hat{x}_1(k_M+1) \\ \hat{x}_2(k_M+1) \\ \hat{x}_3(k_M+1) \end{bmatrix} = \begin{bmatrix} 0.9741 & 0.0244 & 0.0 \\ -0.0975 & 0.9741 & 0.0 \\ 0.0444 & 0.1000 & 1.0 \end{bmatrix} \begin{bmatrix} \hat{x}_1(k_M) \\ \hat{x}_2(k_M) \\ \hat{x}_3(k_M) \end{bmatrix} + \begin{bmatrix} 0.1006 \\ 0.1432 \\ 0.0598 \end{bmatrix} \begin{bmatrix} u(k_M) \end{bmatrix} +$$

$$\begin{bmatrix} L_{11} \\ L_{21} \\ L_{31} \end{bmatrix} \left\{ \begin{bmatrix} y(k_1) \end{bmatrix} - \begin{bmatrix} 1.0 & 4.0 & 2.0 \end{bmatrix} \begin{bmatrix} \hat{x}_1(k_M) \\ \hat{x}_2(k_M) \\ \hat{x}_3(k_M) \end{bmatrix} \right\}$$

The observer matrix L was calculated using the $\emptyset$ matrix found at the multiple sampling rate. The values of the observer matrix were obtained by using each of the two independent methods described in Appendix B. The solution by the algebraic method of equating coefficients yielded

$$\begin{bmatrix} L_{11} \\ L_{21} \\ L_{31} \end{bmatrix} = \begin{bmatrix} -1.0520 \\ -1.0200 \\ 3.0000 \end{bmatrix}$$

while the solution of the Kalman one-step predictor equations resulted in

$$\begin{bmatrix} L_{11} \\ L_{21} \\ L_{31} \end{bmatrix} = \begin{bmatrix} -0.0945 \\ 0.2397 \\ 0.0950 \end{bmatrix}$$

For comparison purposes, a simulation was performed for a single-rate two-sampler system having the same configuration of Figure 4. With the sampling rate of both samplers equal to 5 samples per second, the discrete-time system equations were

$$\begin{bmatrix} x_1(k_2+1) \\ x_2(k_2+1) \\ x_3(k_2+1) \end{bmatrix} = \begin{bmatrix} 0.8868 & 0.0899 & 0.0 \\ -0.3595 & 0.8868 & 0.0 \\ 0.1145 & 0.3875 & 1.0 \end{bmatrix} \begin{bmatrix} x_1(k_2) \\ x_2(k_2) \\ x_3(k_2) \end{bmatrix} + \begin{bmatrix} 0.4062 \\ 0.4927 \\ 0.3461 \end{bmatrix} \begin{bmatrix} u(k_2) \end{bmatrix}$$

$$\begin{bmatrix} y(k_2) \end{bmatrix} = \begin{bmatrix} 1.0 & 4.0 & 2.0 \end{bmatrix} \begin{bmatrix} x_1(k_2) \\ x_2(k_2) \\ x_3(k_2) \end{bmatrix}$$

$$\begin{bmatrix} u(k_2) \end{bmatrix} = -\begin{bmatrix} 7.0271 & -2.4796 & -1.3092 \end{bmatrix} \begin{bmatrix} \hat{x}_1(k_2) \\ \hat{x}_2(k_2) \\ \hat{x}_3(k_2) \end{bmatrix}$$

$$\begin{bmatrix} \hat{x}_1(k_2+1) \\ \hat{x}_2(k_2+1) \\ \hat{x}_3(k_2+1) \end{bmatrix} = \begin{bmatrix} 0.8868 & 0.0899 & 0.0 \\ -0.3595 & 0.8868 & 0.0 \\ 0.1145 & 0.3875 & 1.0 \end{bmatrix} \begin{bmatrix} \hat{x}_1(k_2) \\ \hat{x}_2(k_2) \\ \hat{x}_3(k_2) \end{bmatrix} + \begin{bmatrix} 0.4062 \\ 0.4927 \\ 0.3461 \end{bmatrix} \begin{bmatrix} u(k_2) \end{bmatrix} + \begin{bmatrix} -0.0544 \\ 0.2310 \\ 0.1645 \end{bmatrix} \left\{ \begin{bmatrix} y(k_2) \end{bmatrix} - \begin{bmatrix} 1.0 & 4.0 & 2.0 \end{bmatrix} \begin{bmatrix} \hat{x}_1(k_2) \\ \hat{x}_2(k_2) \\ \hat{x}_3(k_2) \end{bmatrix} \right\}$$

This observer matrix L was developed by the Kalman one-step predictor method discussed in Appendix B. Appendix C demonstrates the procedure followed to determine whether the states of the system are controllable and observable.

The state response of each of these systems is shown in Figure 6 through 14. In these figures, part (a) represents the response of each state variable, x. Part (b) of the figures represents the response of the estimate, $\hat{x}$, of each state variable. The difference between each state vector and its estimate is displayed in part (c) of the figures.

B. Systems With Three Samplers

Consider the three-sampler system shown in Figure 15, which has one input variable but two output variables. First consider the case where the two output variables are each sampled at a different rate. Such a system may arise in certain applications when some portions of the output cannot be sampled at the same rate as other portions due to the characteristics of the measurement devices.

The particular system design considered was one where sampler two and sampler three operate at the same rate — 5 samples per second. The rate of sampler one is again chosen to be 4 samples per second, so the multiple sampling rate remains 20 samples per second. Therefore both u_{k_2} and $y2_{k_2}$ are updated at the faster rate while $y1_{k_1}$ is updated at the slower rate.

Similar to the two-sampler multirate case, $\emptyset$ and T were computed at the multiple sampling rate. The gain matrix H was computed at the rate of sampler three, which in this particular system is the same as the rate of sampler two. Therefore the values of $\emptyset$, T, and H were identical to those used in the two-sampler multirate case. Although the observer matrix L still depends on the $\emptyset$ matrix found at the multiple sampling rate, the calculations necessary to determine the values of L were much more involved since L must now be

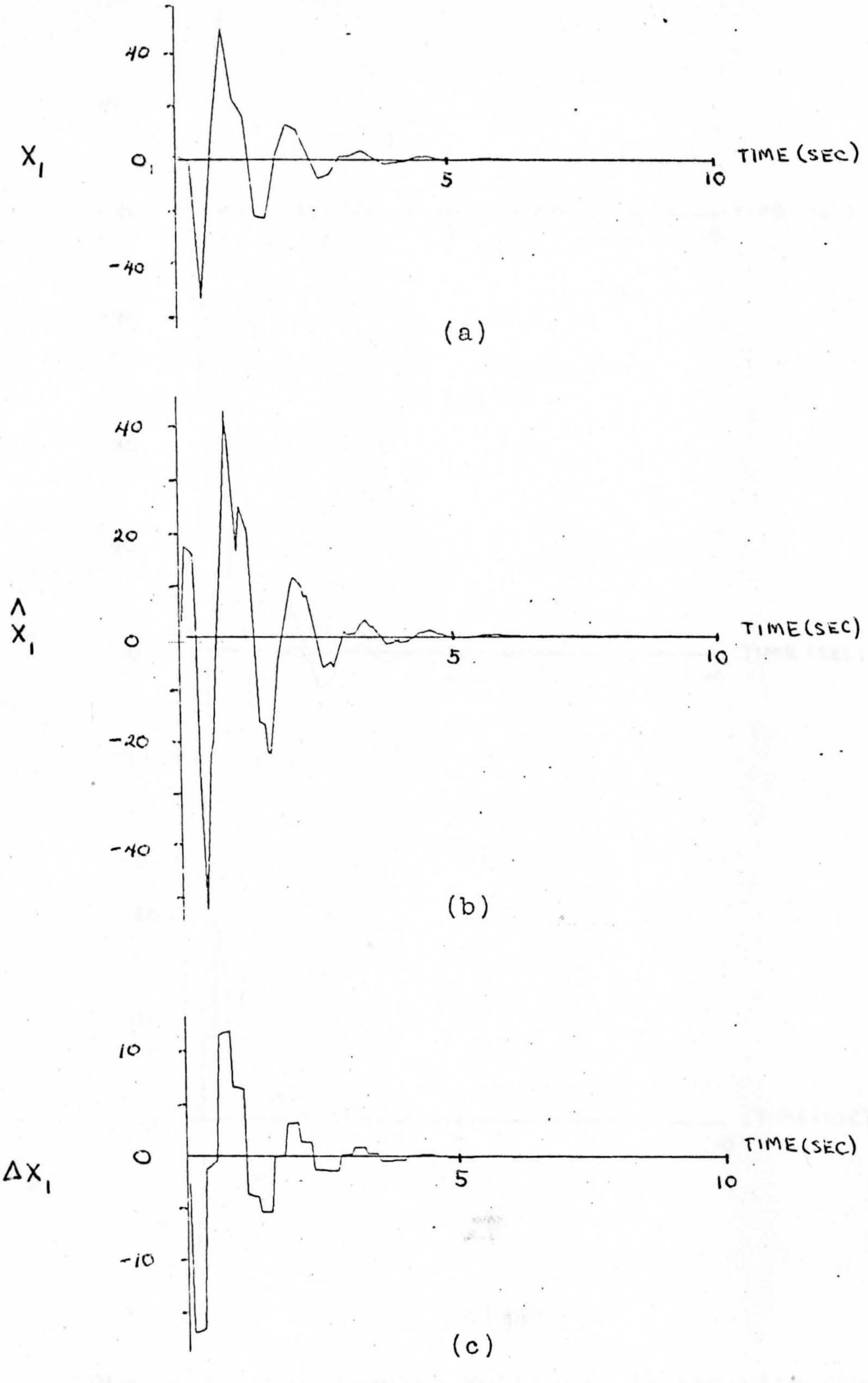

Figure 6. Two-Sampler Multirate System With Observer Values Determined Algebraically.

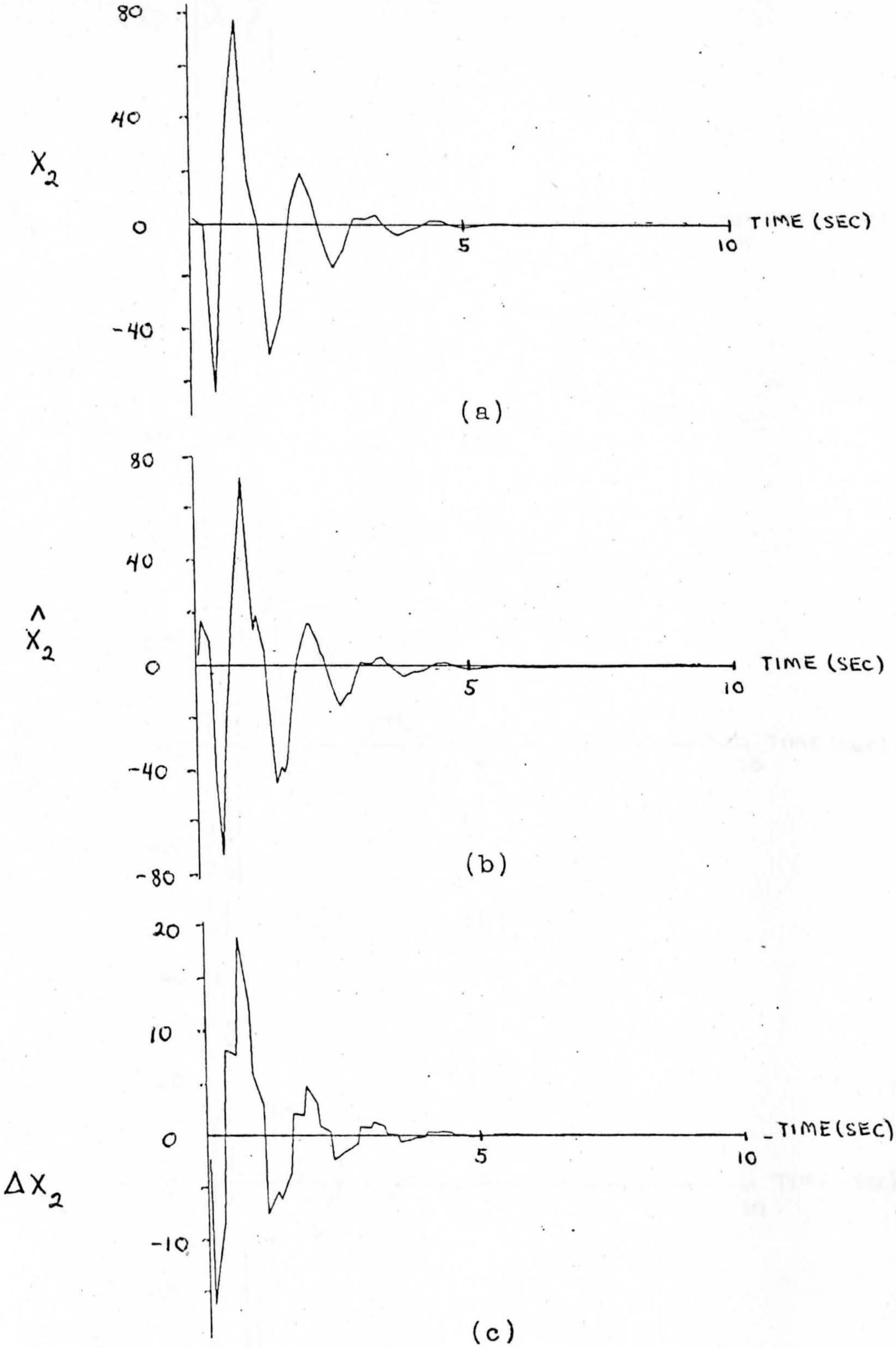

Figure 7. Two-Sampler Multirate System With Observer Values Determined Algebraically.

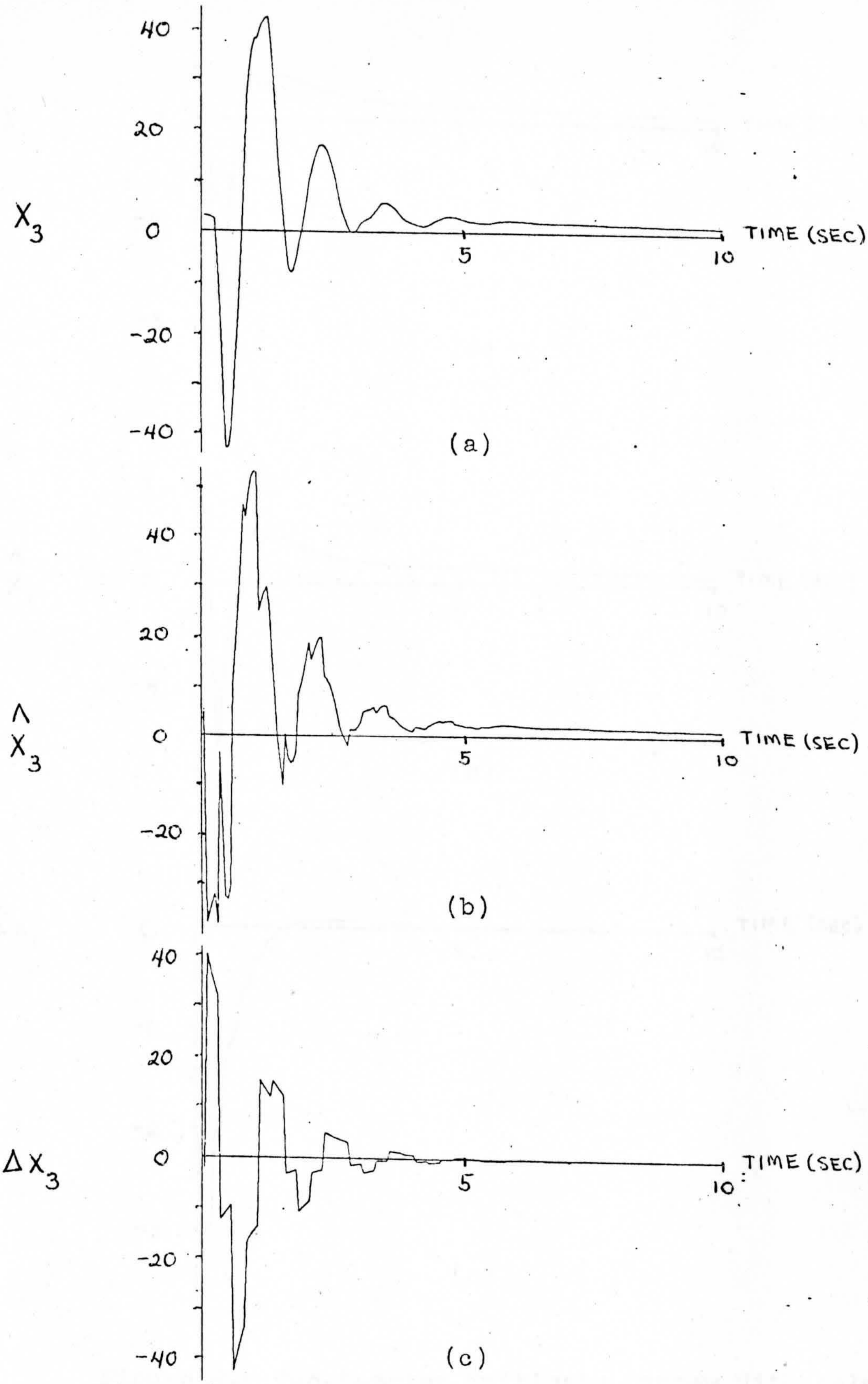

Figure 8. Two-Sampler Multirate System With Observer Values Determined Algebraically.

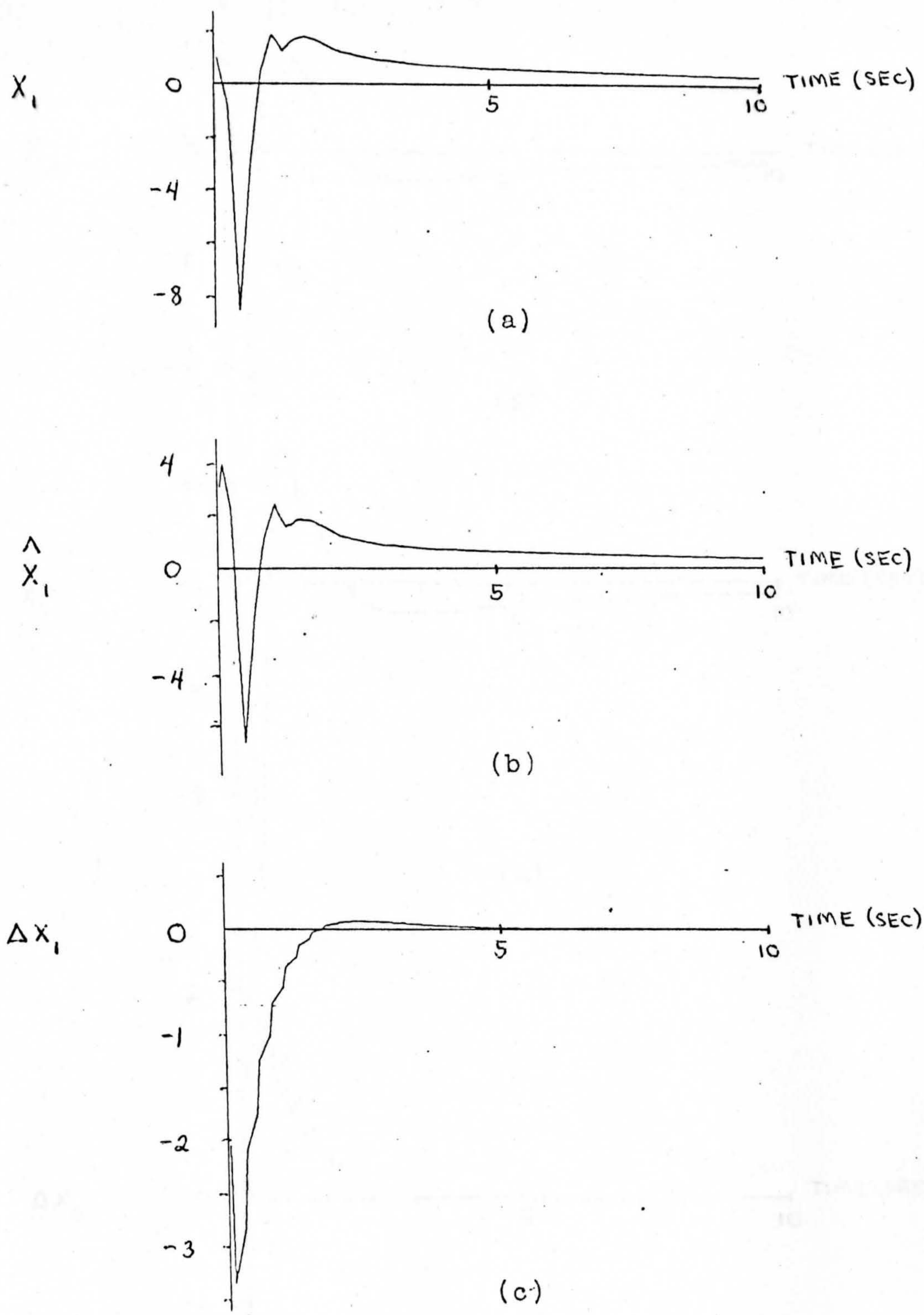

Figure 9. Two-Sampler Multirate System With Kalman One-Step Predictor.

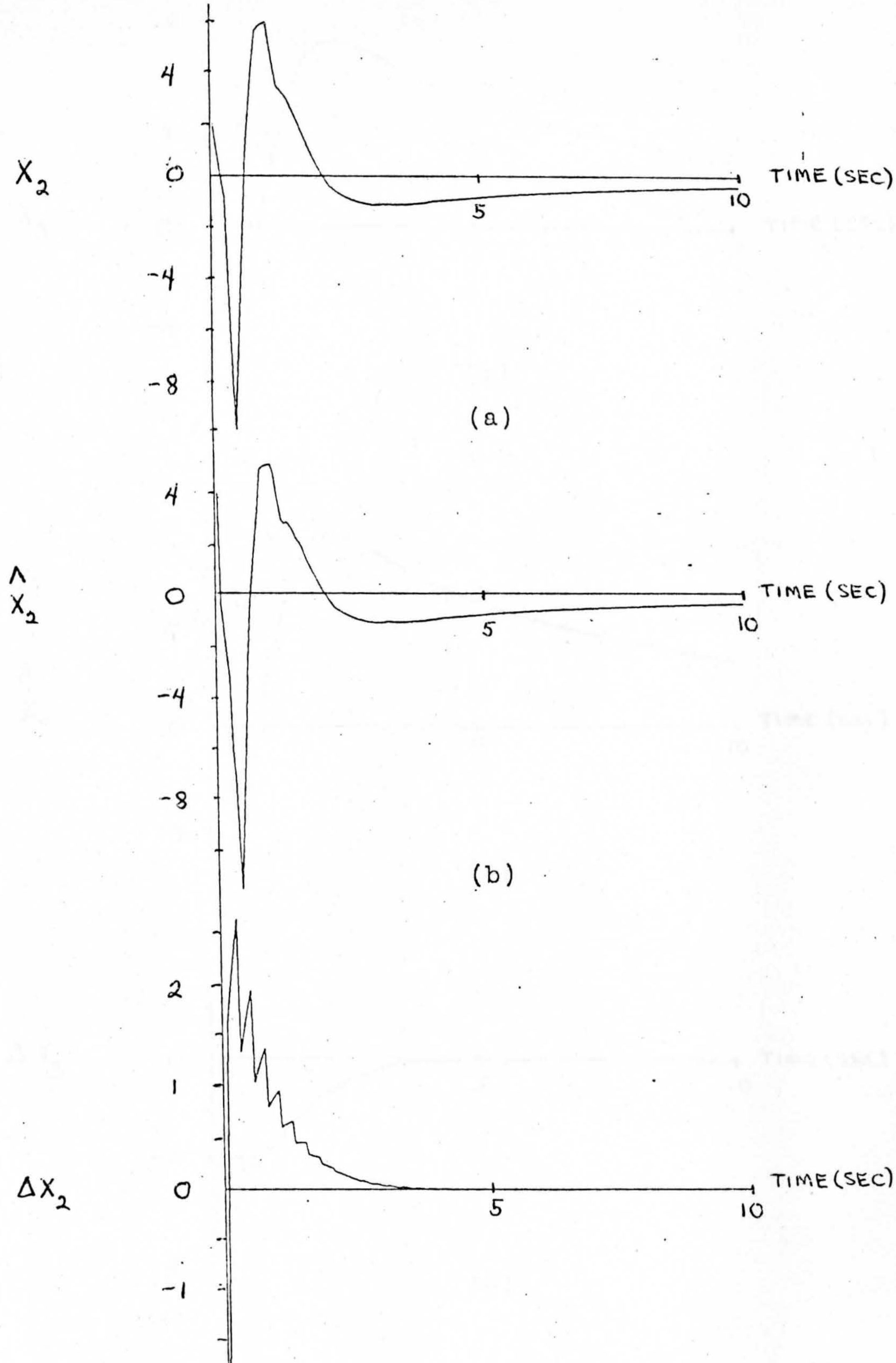

Figure 10. Two-Sampler Multirate System With Kalman One-Step Predictor.

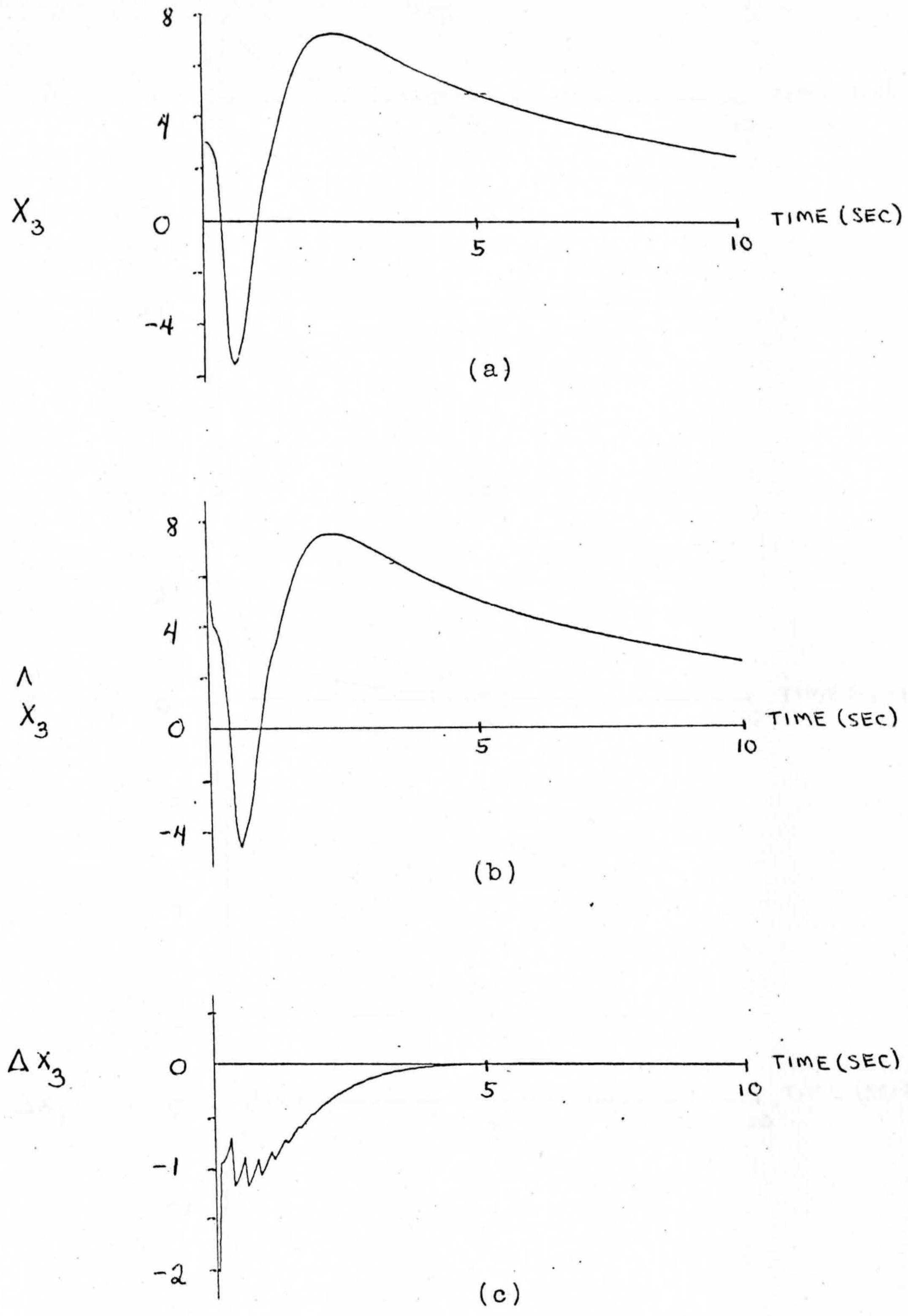

Figure 11. Two-Sampler Multirate System With Kalman One-Step Predictor.

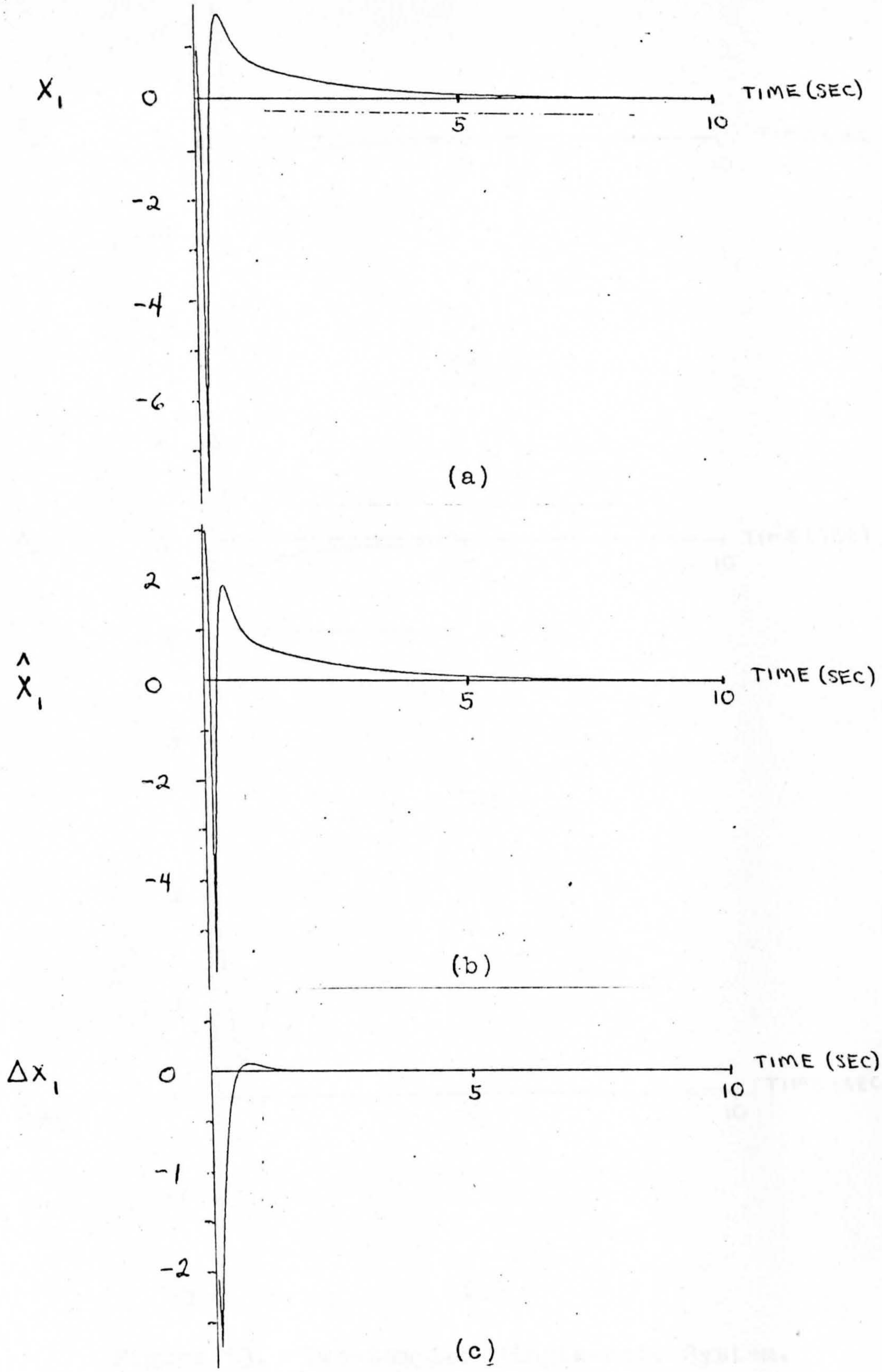

Figure 12. Two-Sampler Single-Rate System.

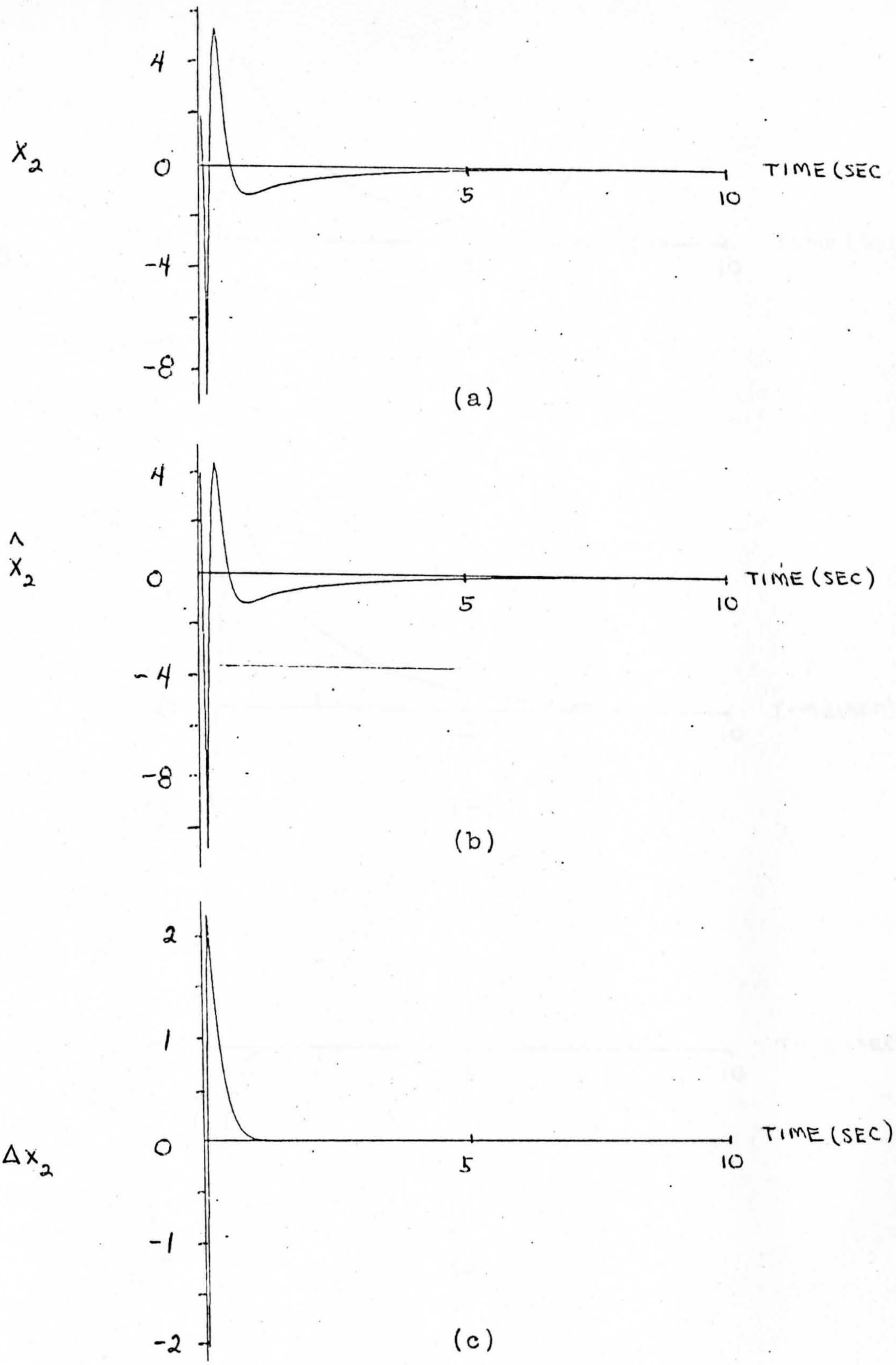

Figure 13. Two-Sampler Single-Rate System.

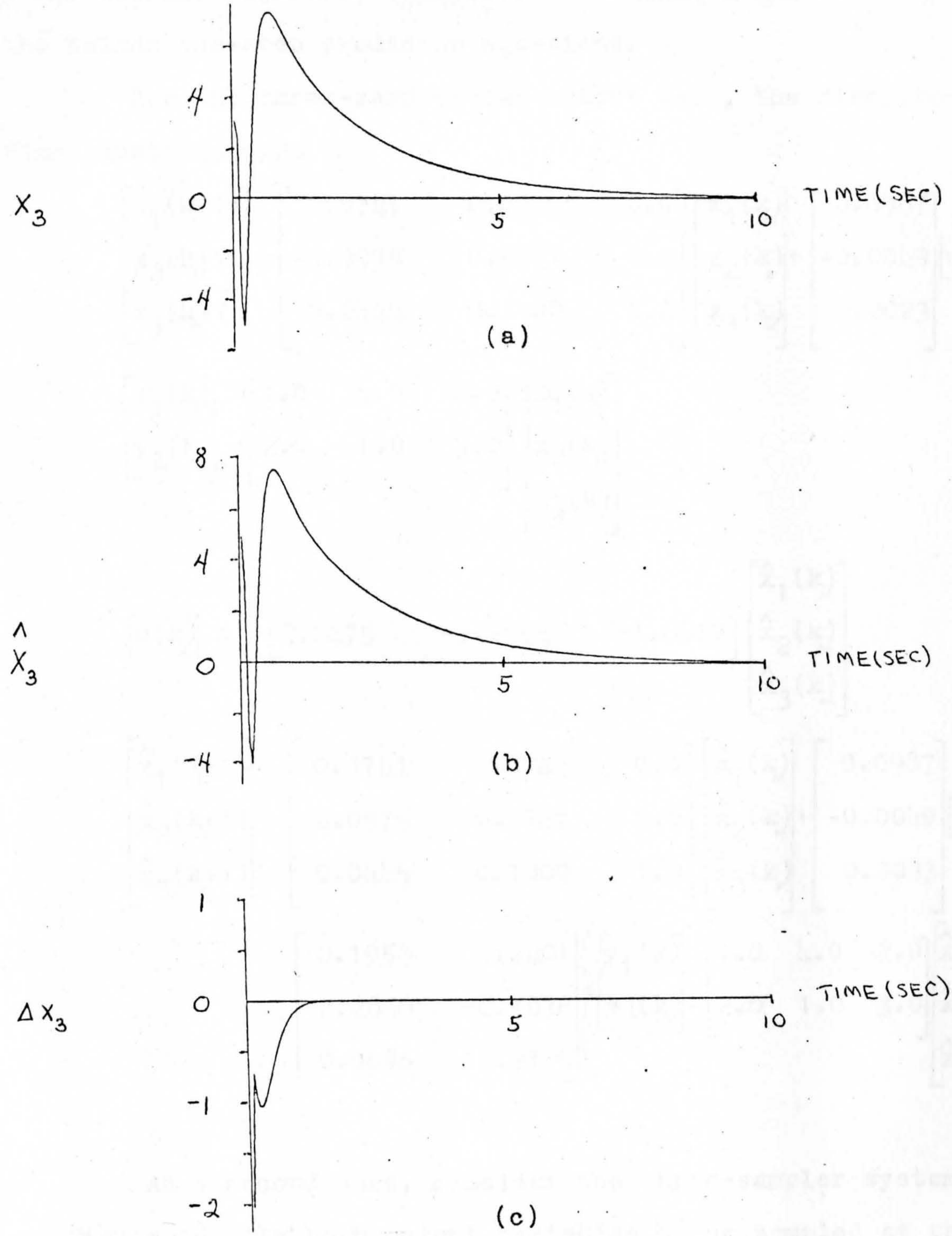

Figure 14. Two-Sampler Single-Rate System.

a 2x3 matrix. Therefore the observer matrix L was found by the Kalman one-step predictor equations.

For the three-sampler two-output case, the discrete-time equations were

$$\begin{bmatrix} x_1(k_M+1) \\ x_2(k_M+1) \\ x_3(k_M+1) \end{bmatrix} = \begin{bmatrix} 0.9741 & 0.0244 & 0.0 \\ -0.0975 & 0.9741 & 0.0 \\ 0.0444 & 0.1000 & 1.0 \end{bmatrix} \begin{bmatrix} x_1(k_M) \\ x_2(k_M) \\ x_3(k_M) \end{bmatrix} + \begin{bmatrix} 0.0987 \\ -0.0049 \\ 0.0023 \end{bmatrix} \begin{bmatrix} u(k_M) \end{bmatrix}$$

$$\begin{bmatrix} y_1(k_1) \\ y_2(k_2) \end{bmatrix} = \begin{bmatrix} 1.0 & 4.0 & 2.0 \\ 2.0 & 1.0 & 3.0 \end{bmatrix} \begin{bmatrix} x_1(k_M) \\ x_2(k_M) \\ x_3(k_M) \end{bmatrix}$$

$$\begin{bmatrix} u(k_3) \end{bmatrix} = -\begin{bmatrix} 2.2475 & -3.2054 & -1.6827 \end{bmatrix} \begin{bmatrix} \hat{x}_1(k_M) \\ \hat{x}_2(k_M) \\ \hat{x}_3(k_M) \end{bmatrix}$$

$$\begin{bmatrix} \hat{x}_1(k_M+1) \\ \hat{x}_2(k_M+1) \\ \hat{x}_3(k_M+1) \end{bmatrix} = \begin{bmatrix} 0.9741 & 0.0244 & 0.0 \\ -0.0975 & 0.9741 & 0.0 \\ 0.0444 & 0.1000 & 1.0 \end{bmatrix} \begin{bmatrix} \hat{x}_1(k_M) \\ \hat{x}_2(k_M) \\ \hat{x}_3(k_M) \end{bmatrix} + \begin{bmatrix} 0.0987 \\ -0.0049 \\ 0.0023 \end{bmatrix} \begin{bmatrix} u(k_M) \end{bmatrix} +$$

$$\begin{bmatrix} -0.1953 & 0.2401 \\ 0.2850 & -0.1876 \\ 0.0696 & 0.2104 \end{bmatrix} \left\{ \begin{bmatrix} y_1(k_1) \\ y_2(k_2) \end{bmatrix} - \begin{bmatrix} 1.0 & 4.0 & 2.0 \\ 2.0 & 1.0 & 3.0 \end{bmatrix} \begin{bmatrix} \hat{x}_1(k_M) \\ \hat{x}_2(k_M) \\ \hat{x}_3(k_M) \end{bmatrix} \right\}$$

As a second case, consider the three-sampler system of Figure 15 with both output variables being sampled at the same rate — 4 samples per second — while the control input is sampled at a faster rate — 5 samples per second. The discrete-time system equations for this case remain as shown

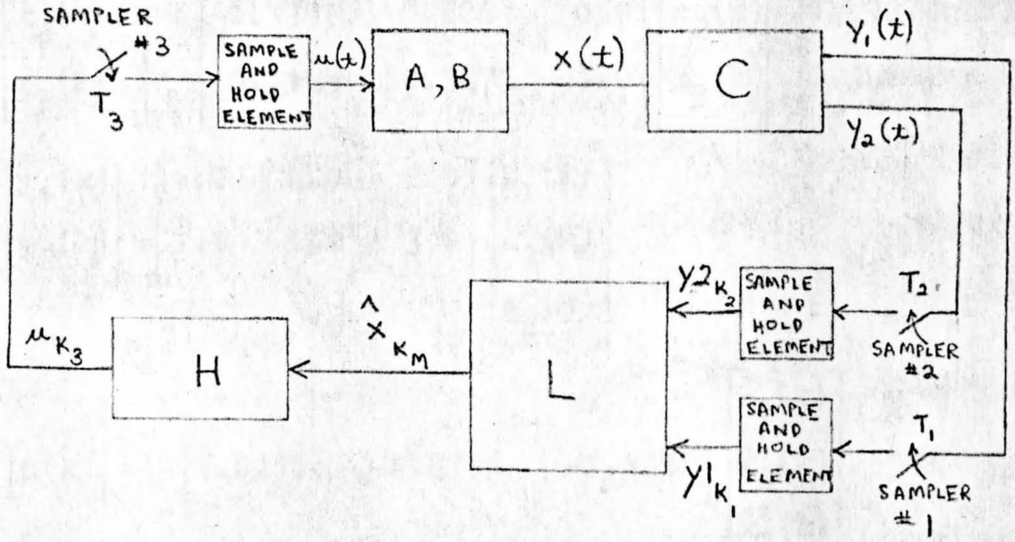

Figure 15. Three-Sampler Multirate System.

above; however both output variables are updated at the slower rate while the control input is still updated at the faster rate.

As before, a simulation was also performed for a single-rate three-sampler system for comparison purposes. With all three samplers in Figure 15 operating at the rate of 5 samples per second, the discrete-time system equations were

$$\begin{bmatrix} x_1(k_2+1) \\ x_2(k_2+1) \\ x_3(k_2+1) \end{bmatrix} = \begin{bmatrix} 0.8868 & 0.0899 & 0.0 \\ -0.3595 & 0.8868 & 0.0 \\ 0.1145 & 0.3875 & 1.0 \end{bmatrix} \begin{bmatrix} x_1(k_2) \\ x_2(k_2) \\ x_3(k_2) \end{bmatrix} + \begin{bmatrix} 0.4062 \\ 0.4927 \\ 0.3461 \end{bmatrix} \begin{bmatrix} u(k_2) \end{bmatrix}$$

$$\begin{bmatrix} y_1(k_2) \\ y_2(k_2) \end{bmatrix} = \begin{bmatrix} 1.0 & 4.0 & 2.0 \\ 2.0 & 1.0 & 3.0 \end{bmatrix} \begin{bmatrix} x_1(k_2) \\ x_2(k_2) \\ x_3(k_2) \end{bmatrix}$$

$$\begin{bmatrix} u(k_2) \end{bmatrix} = -\begin{bmatrix} 7.0271 & -2.4796 & -1.3092 \end{bmatrix} \begin{bmatrix} \hat{x}_1(k_2) \\ \hat{x}_2(k_2) \\ \hat{x}_3(k_2) \end{bmatrix}$$

$$\begin{bmatrix} \hat{x}_1(k_2+1) \\ \hat{x}_2(k_2+1) \\ \hat{x}_3(k_2+1) \end{bmatrix} = \begin{bmatrix} 0.8868 & 0.0899 & 0.0 \\ -0.3595 & 0.8868 & 0.0 \\ 0.1145 & 0.3875 & 1.0 \end{bmatrix} \begin{bmatrix} \hat{x}_1(k_2) \\ \hat{x}_2(k_2) \\ \hat{x}_3(k_2) \end{bmatrix} + \begin{bmatrix} 0.4062 \\ 0.4927 \\ 0.3461 \end{bmatrix} \begin{bmatrix} u(k_2) \end{bmatrix} +$$

$$\begin{bmatrix} -0.1384 & 0.1816 \\ 0.3102 & -0.2315 \\ 0.1202 & 0.1957 \end{bmatrix} \left\{ \begin{bmatrix} y_1(k_2) \\ y_2(k_2) \end{bmatrix} - \begin{bmatrix} 1.0 & 4.0 & 2.0 \\ 2.0 & 1.0 & 3.0 \end{bmatrix} \begin{bmatrix} \hat{x}_1(k_2) \\ \hat{x}_2(k_2) \\ \hat{x}_3(k_2) \end{bmatrix} \right\}$$

In an attempt to improve the system response, the case where the two output variables were each sampled at a different rate was reconsidered. The simulation program for the system was based on y_1 being sampled at time T_1 and y_2 being sampled at T_2. In the previously discussed approach (Case 1), at those instants when y_1 is not available, its value is set equal to what it was at the previous sampling time; similarly for y_2. However if neither one of the y components is available, the observer term is set equal to zero. As an alternate approach (Case 2), this simulation program was revised so that when one of the y components is not available its corresponding part of the observer term is set equal to zero, leaving only the part due to the y component that is present. Since the system variables are still being updated at the rates given in Case 1, the discrete-time equations are identical; the only difference between the two cases is in the method used to update the output components.

The state response of each of these systems is shown in Figures 16 through 27. As before, part (a) represents the state variable, part (b) represents the estimate of the state variable, and part (c) displays the difference between each state variable and its estimate.

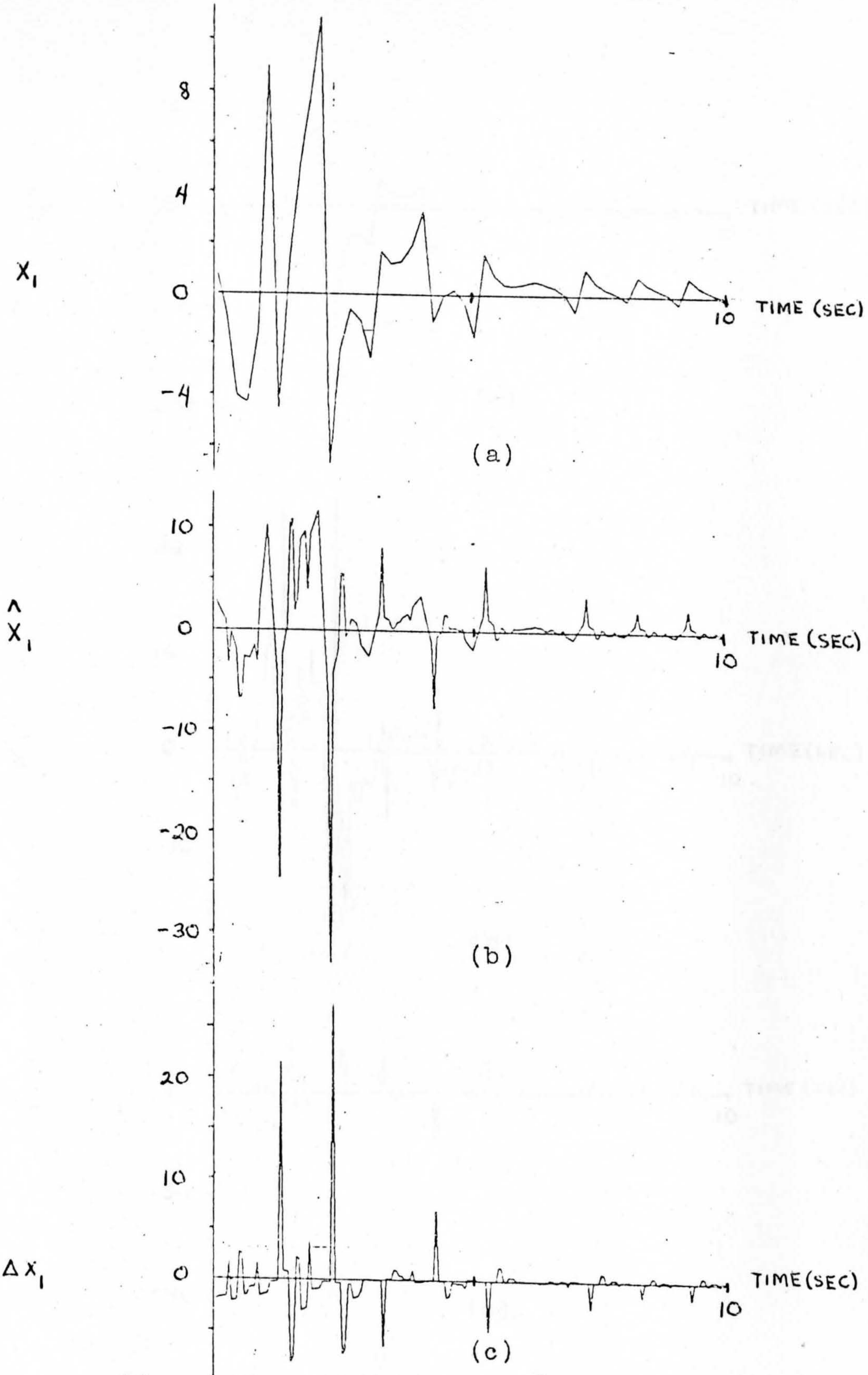

Figure 16. Three-Sampler Multirate System With Outputs Being Sampled at Different Rates (Case 1).

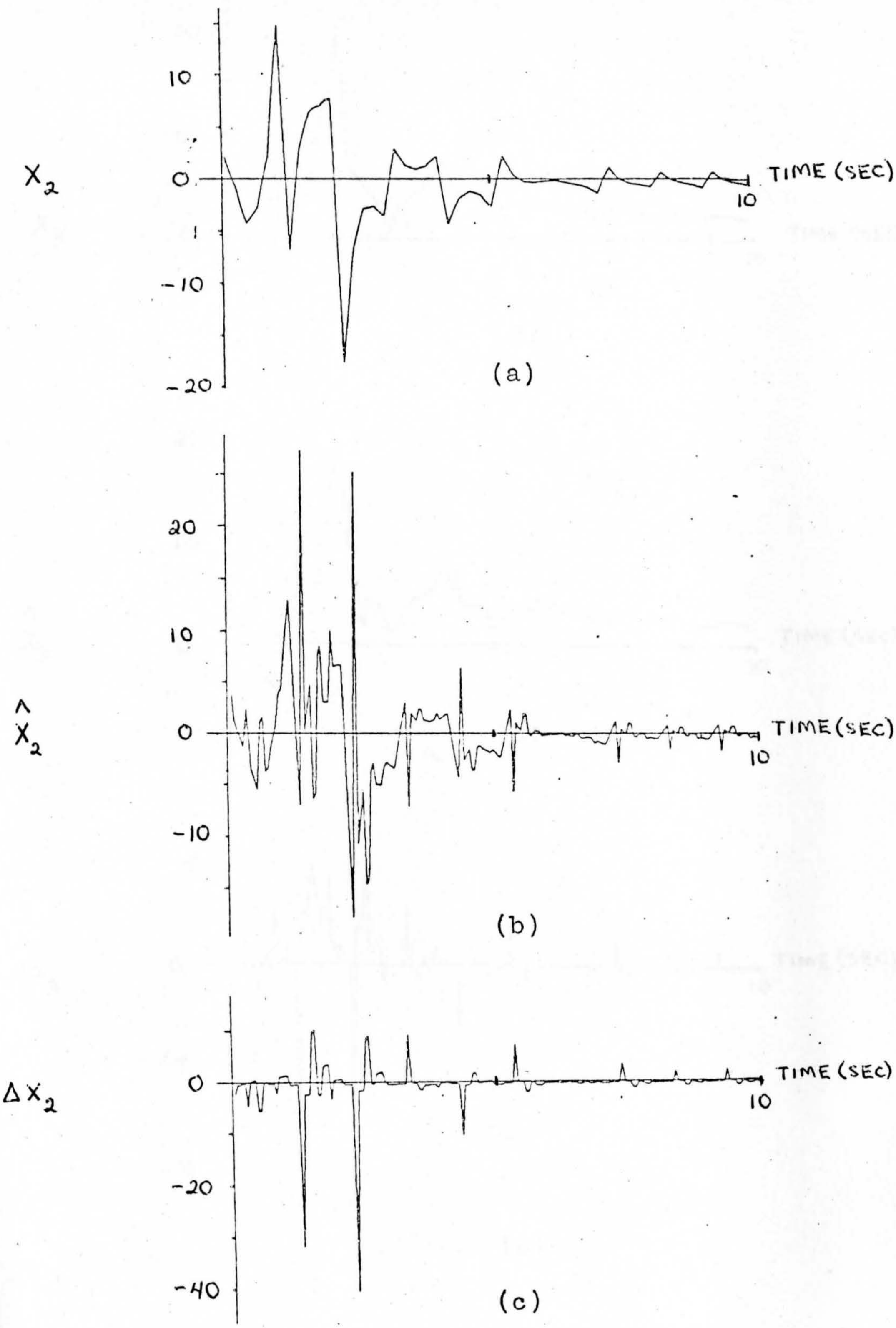

Figure 17. Three-Sampler Multirate System With Outputs Being Sampled at Different Rates (Case 1).

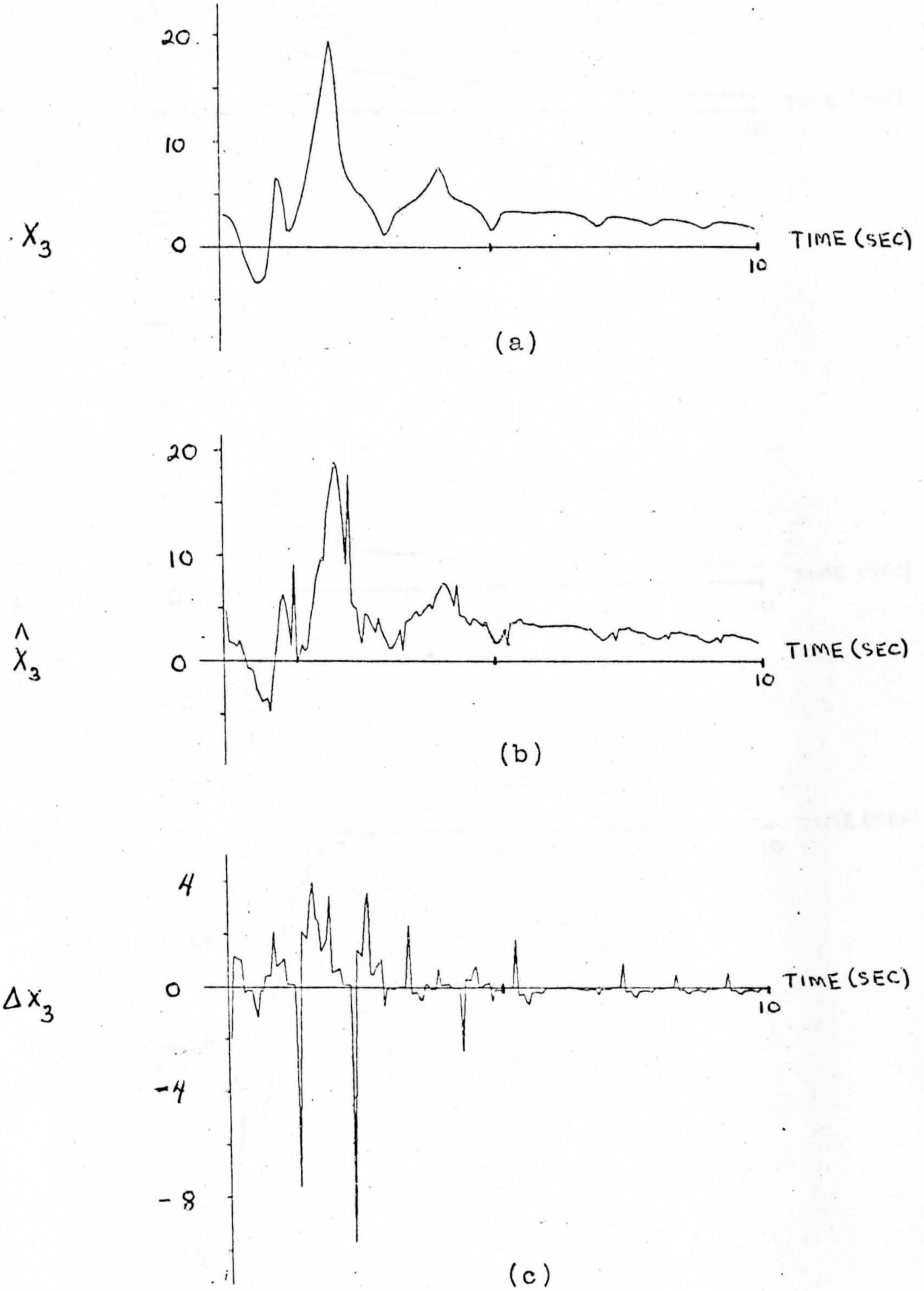

Figure 18. Three-Sampler Multirate System With Outputs Being Sampled at Different Rates (Case 1).

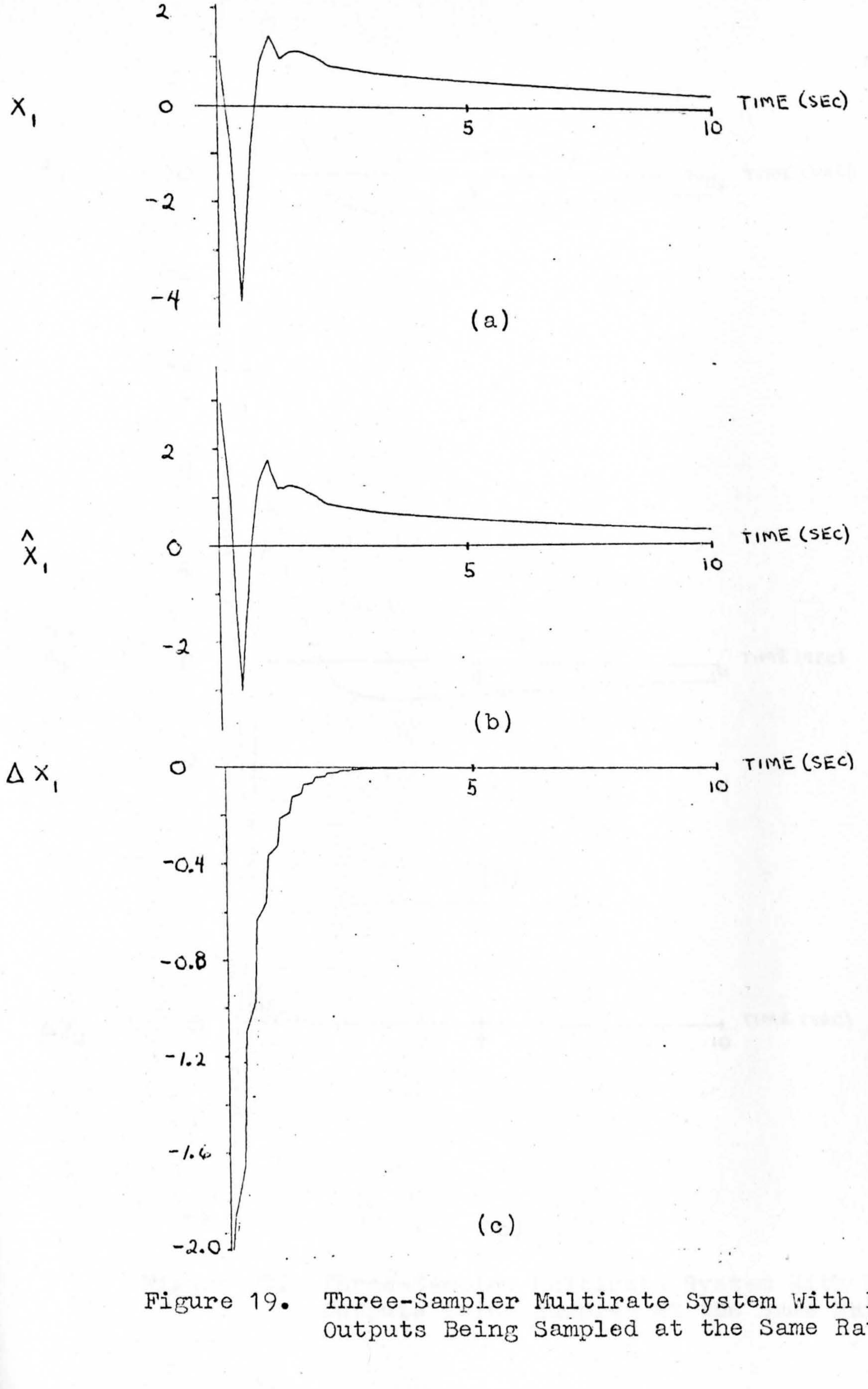

Figure 19. Three-Sampler Multirate System With Both Outputs Being Sampled at the Same Rate.

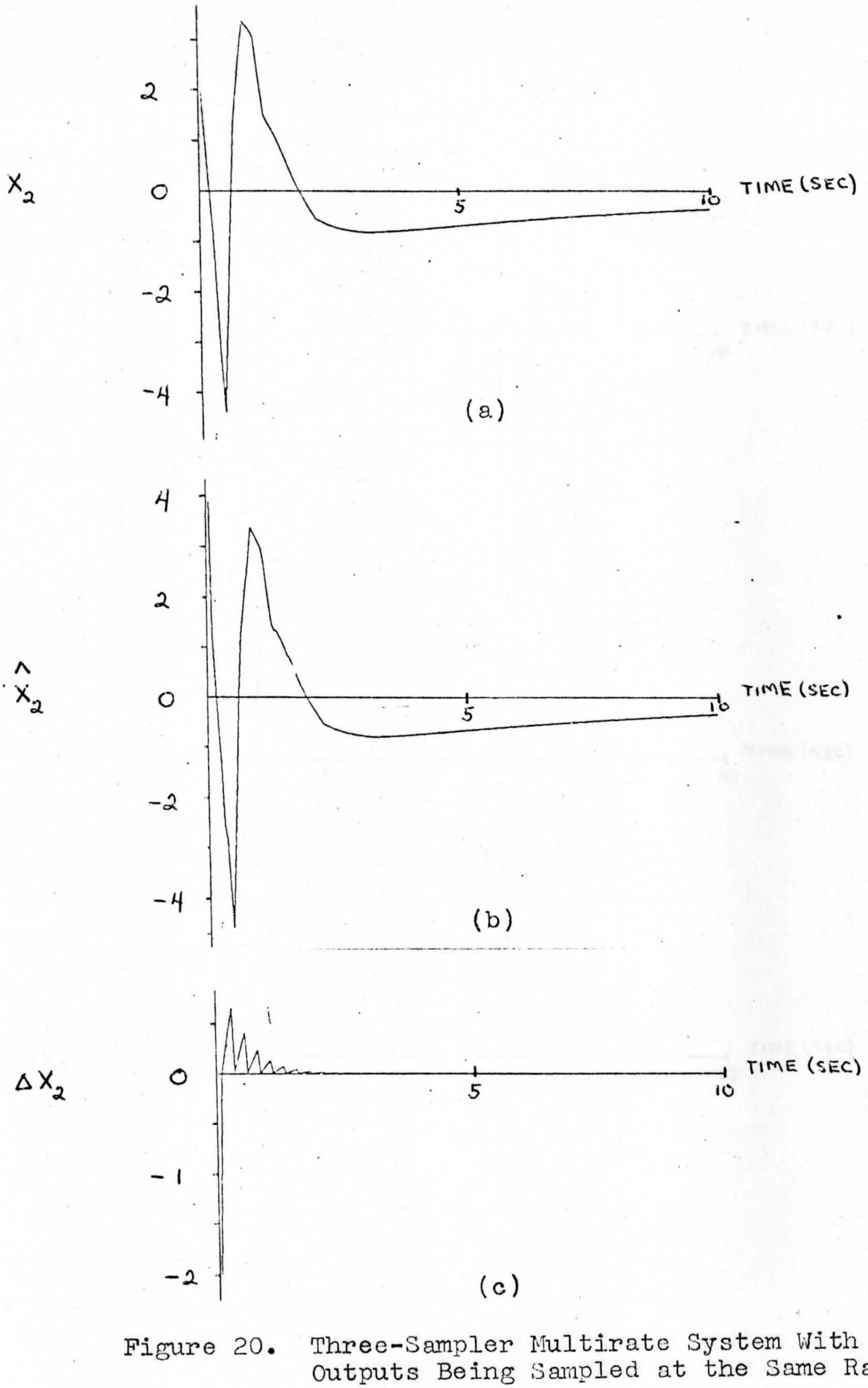

Figure 20. Three-Sampler Multirate System With Both Outputs Being Sampled at the Same Rate.

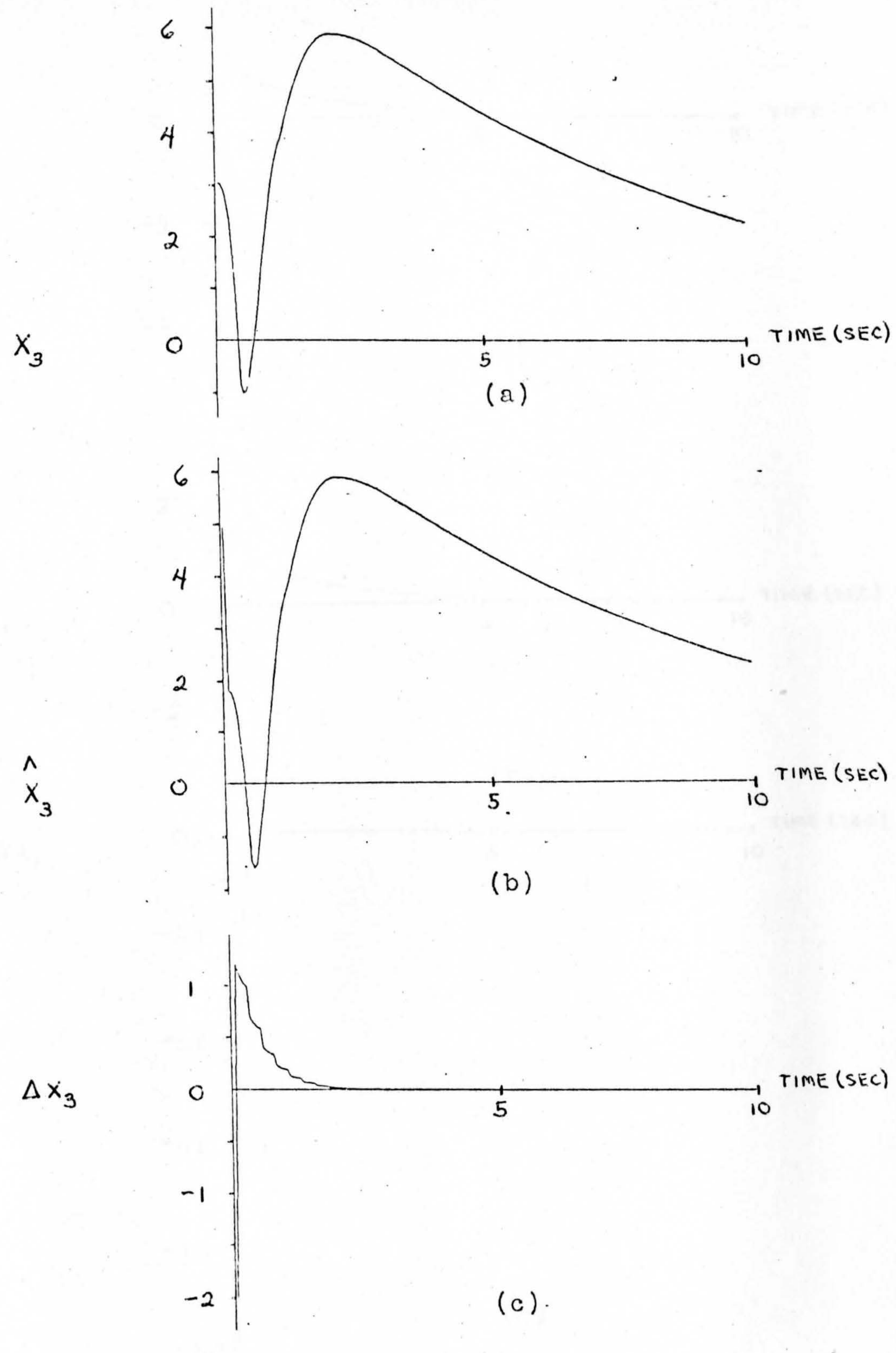

Figure 21. Three-Sampler Multirate System With Both Outputs Being Sampled at the Same Rate.

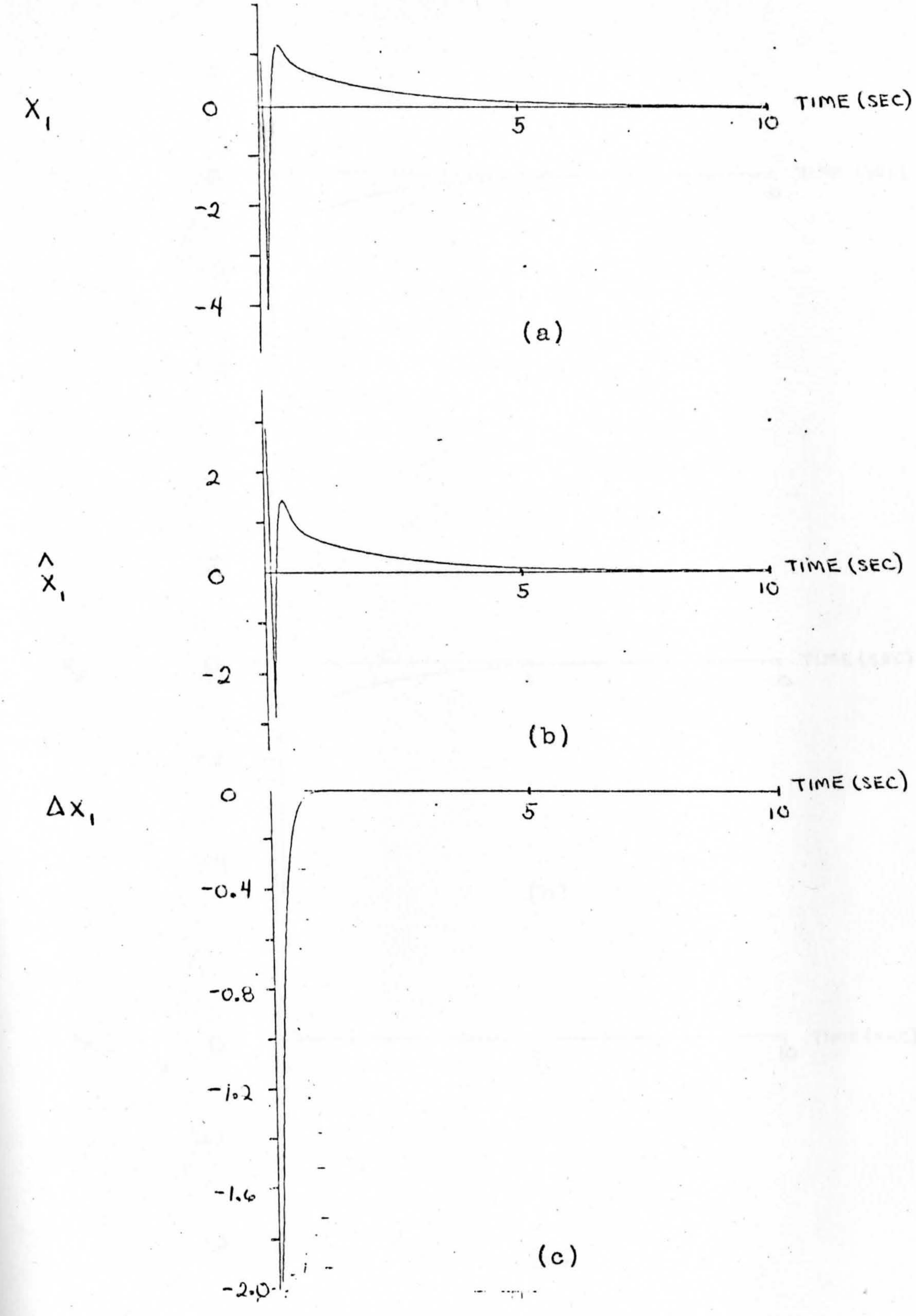

Figure 22. Three-Sampler Single-Rate System.

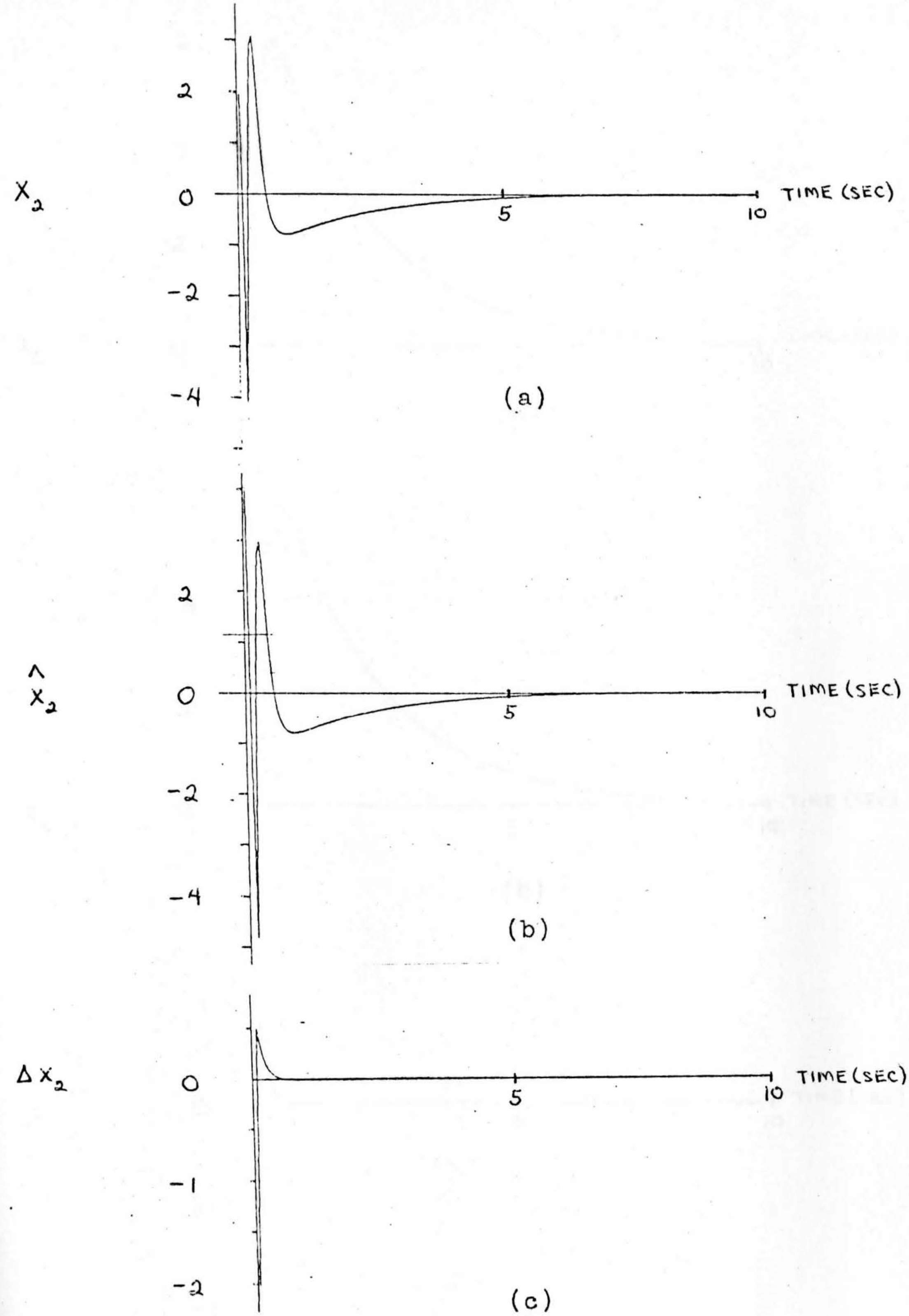

Figure 23. Three-Sampler Single-Rate System.

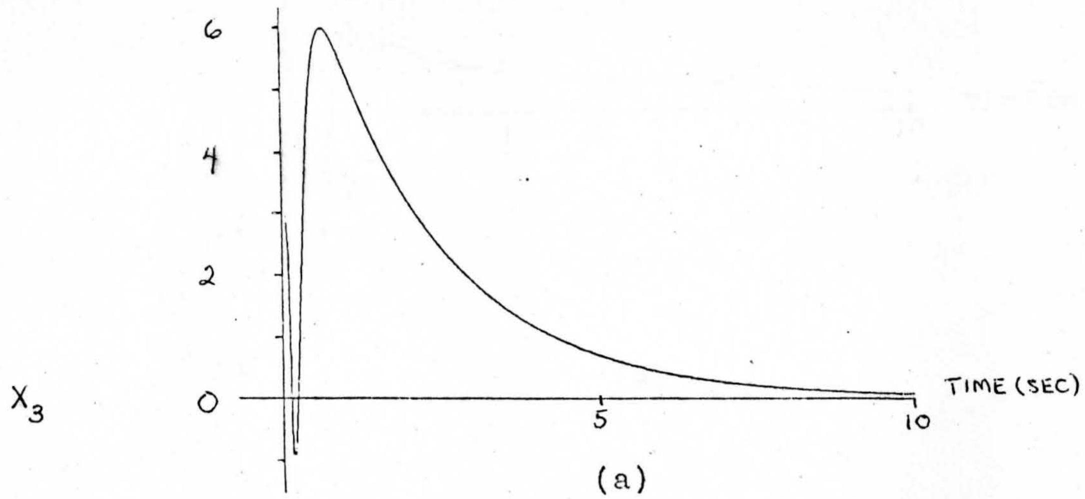

(a)

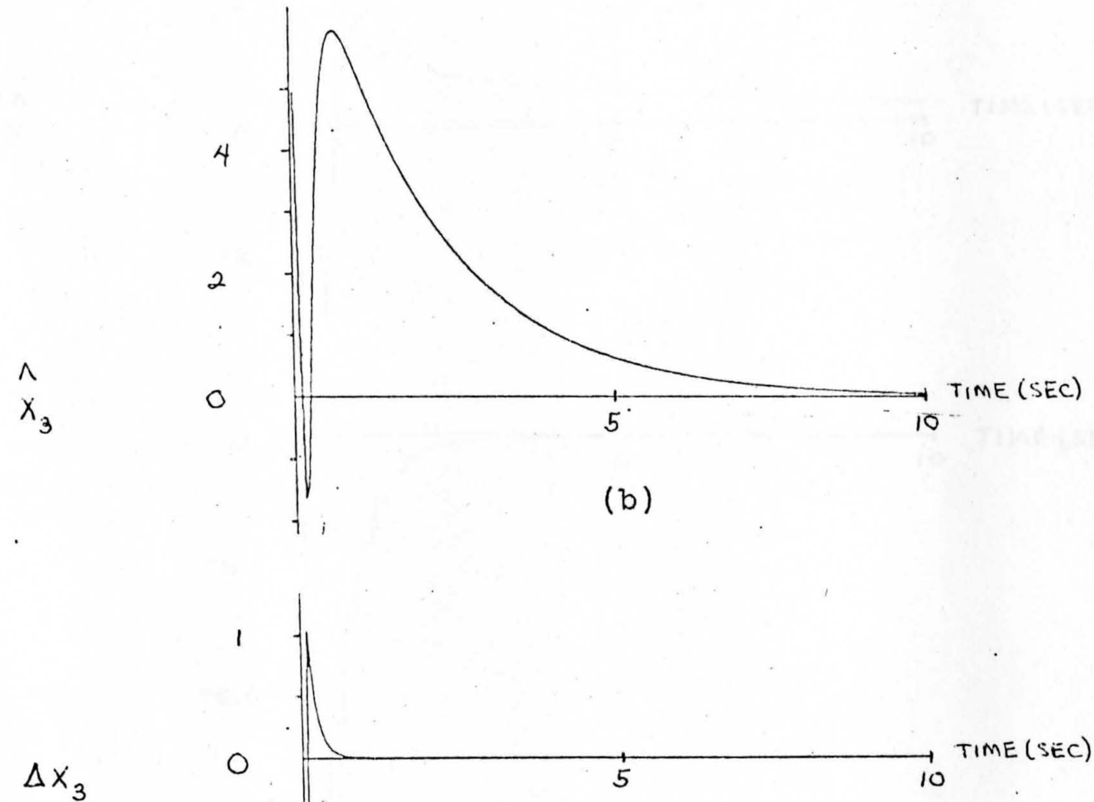

(b)

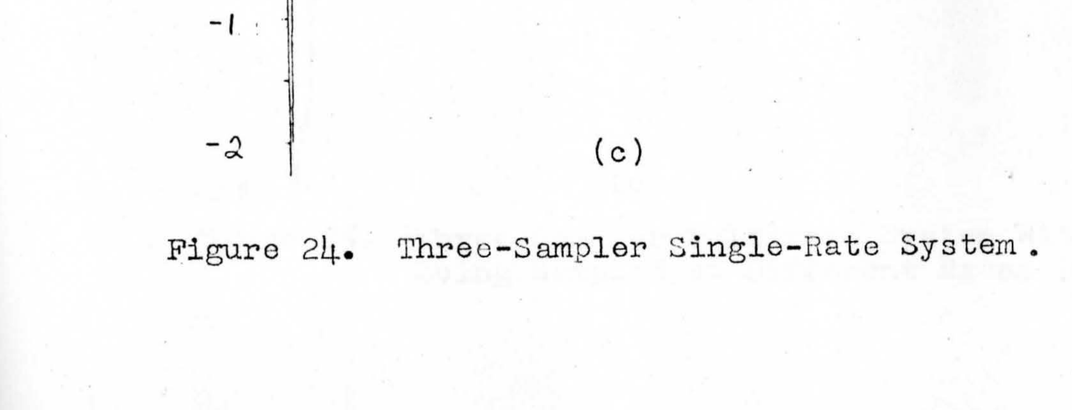

(c)

Figure 24. Three-Sampler Single-Rate System.

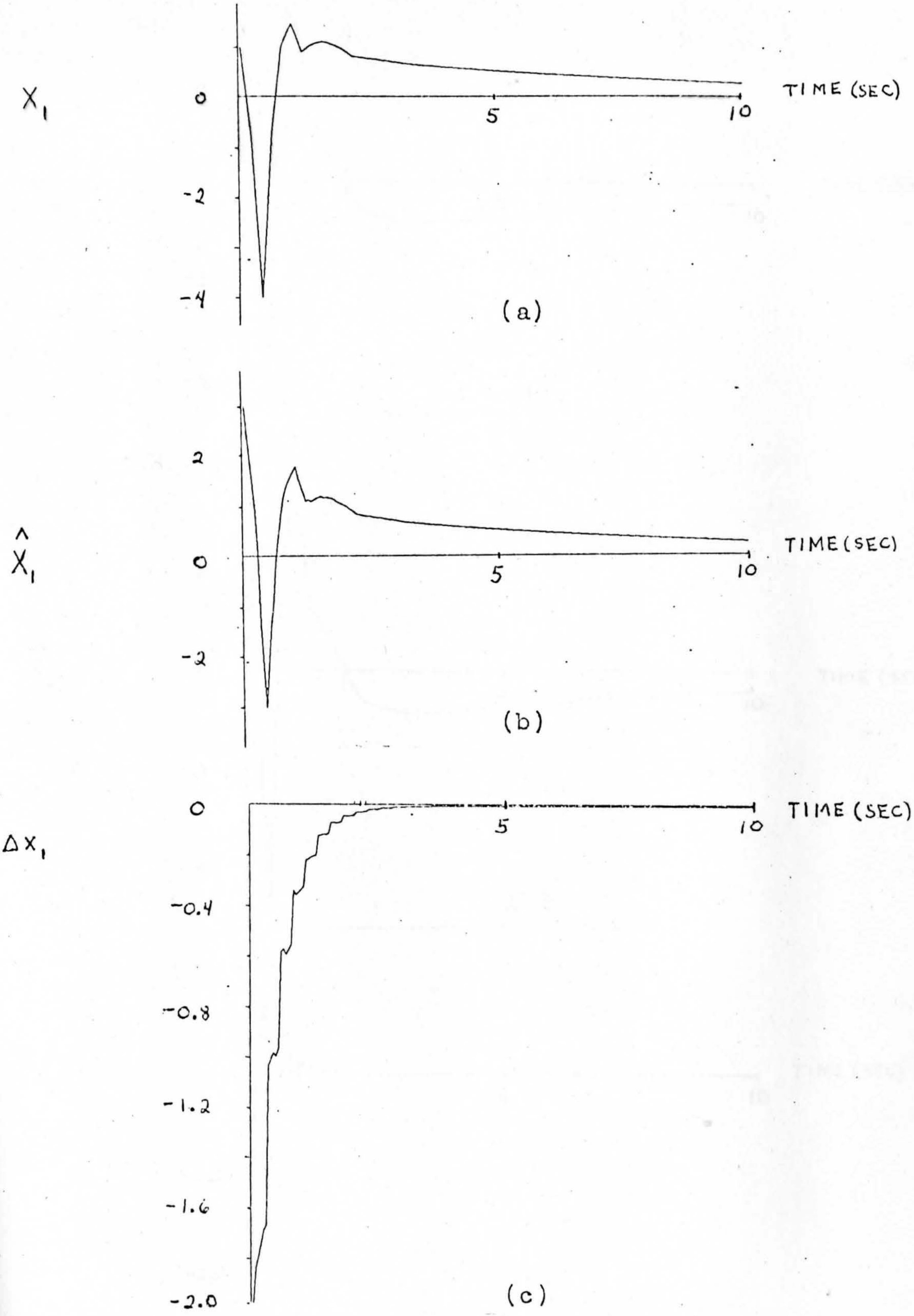

Figure 25. Three-Sampler Multirate System With Outputs Being Sampled at Different Rates (Case 2).

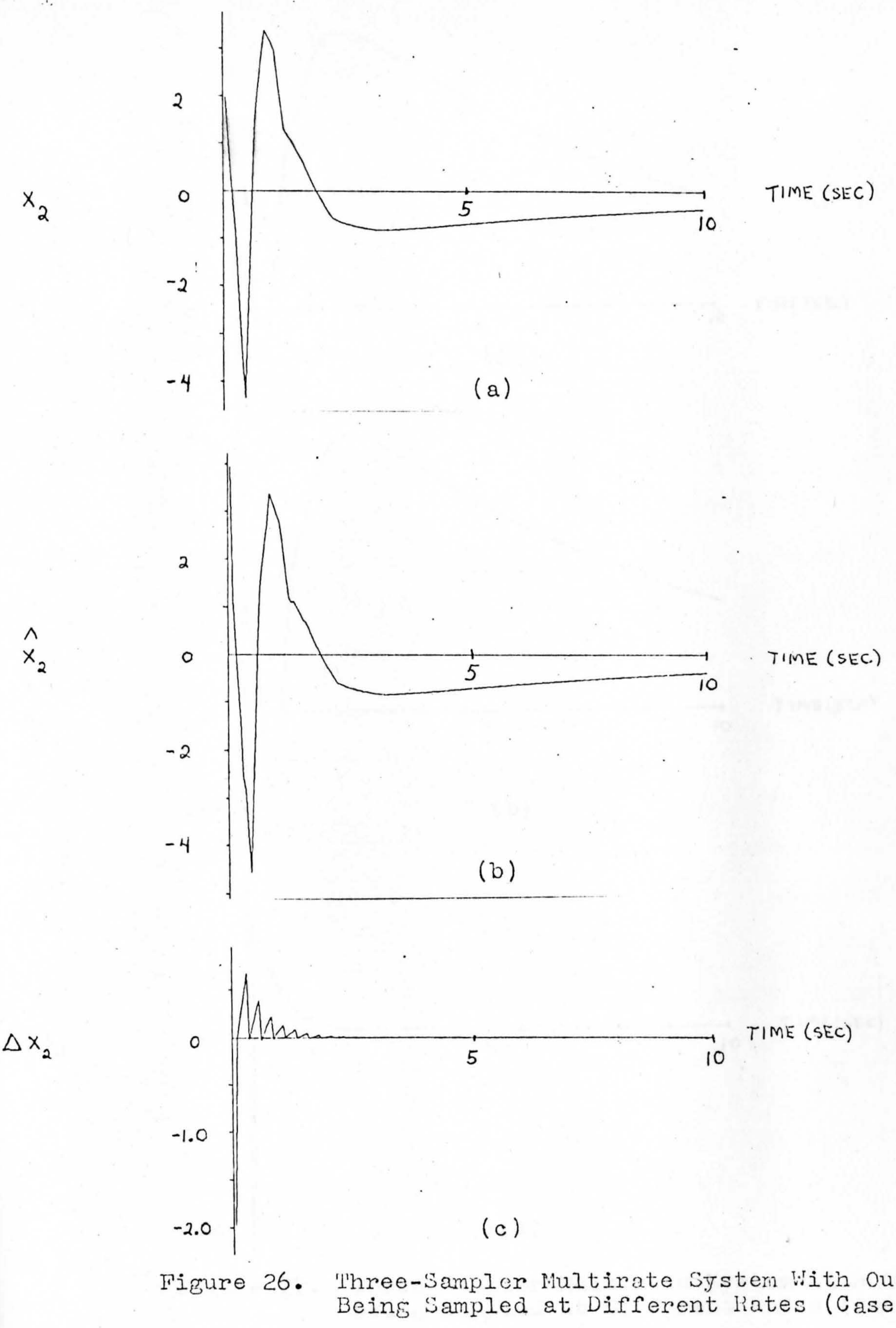

Figure 26. Three-Sampler Multirate System With Outputs Being Sampled at Different Rates (Case 2).

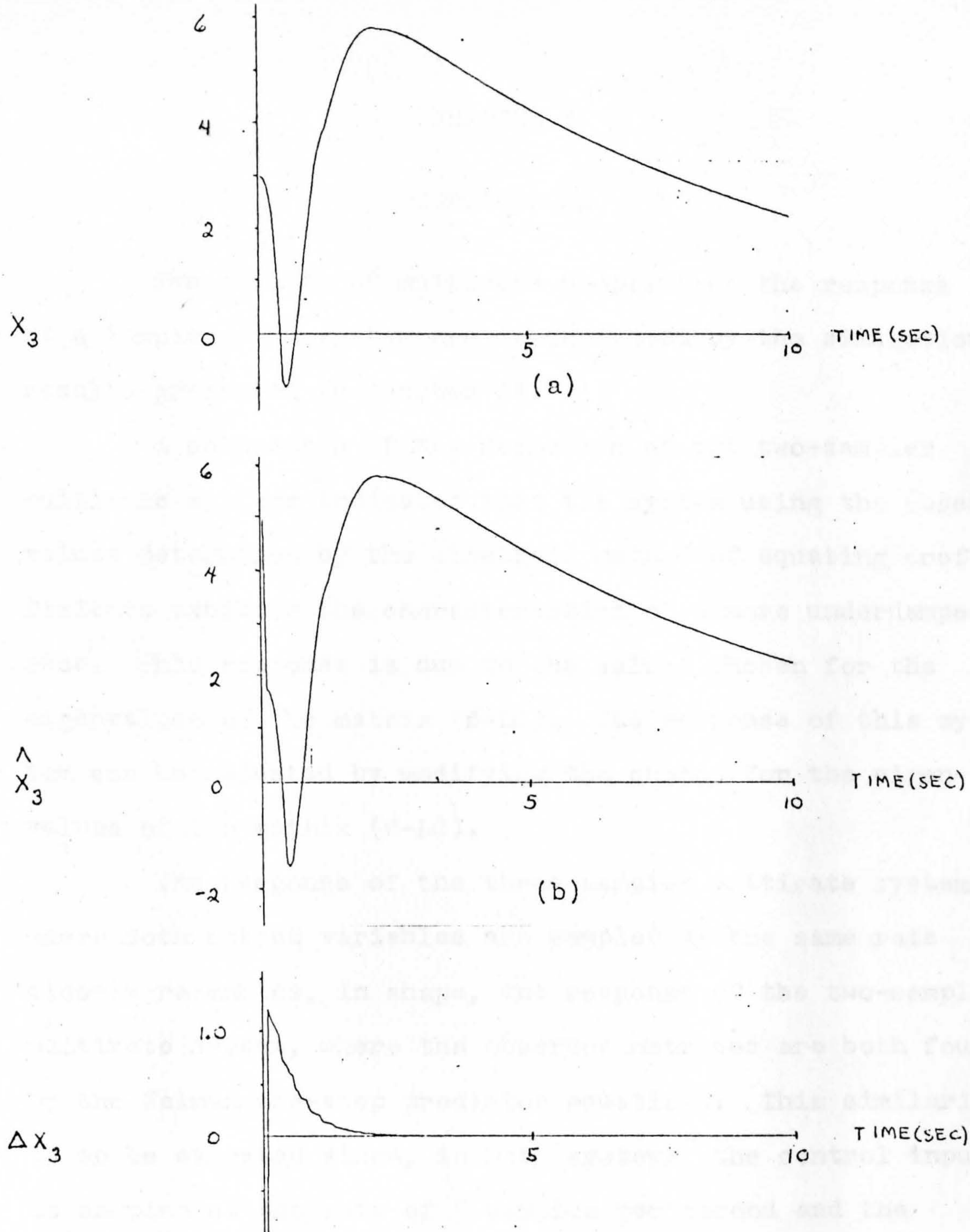

Figure 27. Three-Sampler Multirate System With Outputs Being Sampled at Different Rates (Case 2).

CHAPTER V

CONCLUSIONS

The effects of multirate sampling on the response of a sampled-data system are demonstrated by the simulation results presented in Chapter IV.

A comparison of the responses of the two-sampler multirate systems indicates that the system using the observer values determined by the algebraic method of equating coefficients exhibits the characteristics of a more underdamped case. This response is due to the values chosen for the eigenvalues of the matrix (Ø-LC). The response of this system can be adjusted by modifying the choice for the eigenvalues of the matrix (Ø-LC).

The response of the three-sampler multirate system where both output variables are sampled at the same rate closely resembles, in shape, the response of the two-sampler multirate system, where the observer matrices are both found by the Kalman one-step predictor equations. This similarity is to be expected since, in both systems, the control input is sampled at the rate of 5 samples per second and the entire output vector is sampled at the rate of 4 samples per second.

However for the three-sampler multirate system with each of the two output variables sampled at a different rate, the response does not decay to zero as rapidly as the other three-sampler systems. Furthermore, the response contains periodic pulses which, although they decay, account for the lengthening of the response time interval. The simulation program for this system model was based on y_1 being sampled at time T_1 and y_2 being sampled at time T_2. At the sampling instants when y_1 is not sampled, its value was set equal to what it was at the previous sampling time; that is, at the sampling times when y_1 is not updated, it was assumed that

$$y1_{k_1} = y1_{k_1-1}$$

Similarly for y_2. In the calculation of the z terms described by equation (3.2), these values for y_1 and y_2, containing past information, were used.

However, because this simulation exhibited oscillations and required a comparatively long time to decay, the simulation program was revised so that the particular y component which is being updated is the only one that affects the calculation of the z term at that instant. This approach results in a simulation using

$$z_{k_M} = \begin{cases} L_1(y1_{k_1} - C_1\hat{x}_{k_M}) & \text{at } k_M T_M = k_1 T_1 \neq k_2 T_2 \\ L_2(y2_{k_2} - C_2\hat{x}_{k_M}) & \text{at } k_M T_M = k_2 T_2 \neq k_1 T_1 \\ L(y1_{k_1} - C_1\hat{x}_{k_M} + y2_{k_2} - C_2\hat{x}_{k_M}) & \text{at } k_M T_M = k_1 T_1 = k_2 T_2 \\ 0 & \text{at all other times} \end{cases}$$

It can be seen that this system model resulted in a response which converges more rapidly and with less oscillations.

A possibility for further investigation may involve a more detailed study of this three-sampler multirate system with two outputs sampled at different rates. The analysis might consider the application of multirate sampling to systems in which the output can be divided into two subgroups — one subgroup containing components which vary rapidly with time while the other subgroup consists of components which vary more slowly with time. In such a system, the components which change more rapidly would be sampled at the faster rate while the components which change more slowly would be sampled at the slower rate. This approach would insure that a minimum amount of change occurs between successive sampling instants [16].

Further improvement in system response might be accomplished by trial-and-error experimentation in the choice of the weighting matrices Q and R. Although this was done to some extent, further experimentation may be desirable in a practical application. It might also prove interesting to investigate the effects of varying the sampling interval. This was done for the systems described in this thesis with the faster rate maintained at 5 samples per second but the slower rate decreased to 2 samples per second. The system responses for the various cases at these new sampling rates were similar to the responses already presented.

It should also be noted that the responses of the single-rate sampled-data systems indicate that their estimated state vector $\hat{x}$ closely approximates the state variable x. However, it should be realized that the simulation of a single-rate system assumes that measurements of the system variables are available at the faster sampling rate of 5 samples per second. On the other hand, the multirate design assumes that certain measurements are only available at the slower rate of 4 samples per second while the control input u_k is required at a rate of 5 samples per second. In some practical applications of sampled-data systems, the measurement variables are not always available at the same rate as that with which the control input is required. Furthermore, in certain systems, although all the system variables may be available for updating at the same sampling rate, it may be desirable to update some of the variables at a slower rate than the others. This is particularly applicable in systems where certain variables change slower than others. By sampling these variables at a slower rate than the rest of the system, it is possible to reduce the amount of calculations necessary. In such situations, the designer may find that multirate sampling becomes advantageous.

APPENDIX A

Determination of the A Matrix

The A matrix was chosen to insure that the continuous-time system would be stable. This was done by choosing the open-loop system poles in the left-hand plane. For the particular continuous-time systems discussed in Chapter IV, the open-loop poles were chosen to be

$$\lambda_{1,2}=-0.5 \pm j1.0$$

$$\lambda_3=0.0 \quad .$$

These poles yield a characteristic equation

$$0=[\lambda-0][\lambda-(-0.5+j)][\lambda-(-0.5-j)]$$

$$0=\lambda[\lambda^2+\lambda+1.25] \qquad \text{(A-1)}$$

The desired A matrix is of the form

$$A = \begin{bmatrix} a_{11} & a_{12} & a_{13} \\ a_{21} & a_{22} & a_{23} \\ a_{31} & a_{32} & a_{33} \end{bmatrix}$$

For simplicity, a_{13} and a_{23} were chosen to be zero. Therefore the characteristic equation of A is

$$\left|\lambda I-A\right|=0=(\lambda-a_{33})\left[(\lambda-a_{11})(\lambda-a_{22})-a_{12}a_{21}\right]$$

$$0=(\lambda-a_{33})[\lambda^2-\lambda(a_{11}+a_{22})+(a_{11}a_{22}-a_{12}a_{21})] \qquad \text{(A-2)}$$

Equating the coefficients of like terms in equations (A-1) and (A-2) yields

$$a_{33}=0.0 \qquad \text{(A-3)}$$

$$-(a_{11}+a_{22})=1.0 \qquad \text{(A-4)}$$

$$a_{11}a_{22}-a_{12}a_{21}=1.25 \tag{A-5}$$

Choosing a_{22} to be -0.5 in equation (A-4) determines that a_{11} is -0.5. Substituting these values into equation (A-5) and selecting a_{12} to be 0.5 determines that a_{21} is -2.0. The values of a_{31} and a_{32} are thus found to be arbitrary and were selected to have values of 1.0 and 2.0 respectively.

Therefore the matrix A which was chosen to be used for the continuous-time systems is

$$A = \begin{bmatrix} -0.5 & 0.5 & 0.0 \\ -2.0 & -0.5 & 0.0 \\ 1.0 & 2.0 & 0.0 \end{bmatrix}$$

APPENDIX B

Determination of the Observer Matrix L

The observer matrix L must be chosen so that the eigenvalues of the matrix $(\emptyset\text{-}LC)$ are within the unit circle in the z-plane. As was explained in Section C of Chapter II, the choice of such eigenvalues insures that the state of the observer will converge to that of the observed system. For this reason, the eigenvalues of the matrix $(\emptyset\text{-}LC)$ were chosen to be

$$\lambda_{1,2}=0.8\angle\pm 11^\circ = 0.79\pm j0.15$$

$$\lambda_3 = 0.5$$

These poles yield a characteristic equation

$$0=(\lambda-0.8\angle 11^\circ)(\lambda-0.8\angle -11^\circ)(\lambda-0.5)$$

$$0=\lambda^3-2.10\lambda^2+1.44\lambda-0.32 \tag{B-1}$$

The unknown observer matrix L can be found by equating the coefficients of the determinant $\left|\lambda I-(\emptyset\text{-}LC)\right|$ to the corresponding coefficients of equation (B-1).

An alternate method for determining the unknown observer matrix L is through the use of the Kalman one-step predictor , which is described by the following set of equations [15]

$$L_k=\emptyset P_k C'(CP_kC')^{-1} \tag{B-2}$$

where $$P_{k+1}=\emptyset\left[P_k-P_kC'(CP_kC')^{-1}CP_k\right]\emptyset' \tag{B-3}$$

The observer matrix L can be found through the computer algorithm which determines the solution of equations (B-2) and (B-3). The use of this computer algorithm enables the designer to determine the values of the observer matrix quicker, easier, and more accurately than the previously described algebraic method of equating coefficients. The complexity of the algebraic method increases significantly as the order of the system increases . Even for a third-order case, this fact became apparent as the complexity of the algebraic equations increased tremendously.

APPENDIX C

Checking for Controllability and Observability

Before forming the discrete-time system, a check should be performed on the continuous-time system to insure that it is both controllable and observable. By definition, a system is said to be controllable if all of the state variables can be changed by adjusting the input variables. Also, a system is said to be observable if every state variable can be found from measuring values of the output.

A system is controllable if and only if the matrix

$$P = \left[B \,\vdots\, AB \,\vdots\, A^2B \,\vdots\, \dots \,\vdots\, A^{n-1}B \right]$$

has rank n, where n is the order of the matrix A.

A system is observable if and only if the matrix

$$Q = \left[C' \,\vdots\, A'C' \,\vdots\, (A')^2C' \,\vdots\, \dots \,\vdots\, (A')^{n-1}C' \right]$$

has rank n, where n is the order of the matrix A [17].

REFERENCES

[1] M. Athans and P. Falb, Optimal Control: An Introduction to the Theory and Its Applications. New York: McGraw-Hill Book Company, 1966.

[2] R. E. Kalman and J. E. Bertran, "A Unified Approach to the Theory of Sampling Systems," Jour. Franklin Inst., pp. 405-436, May 1959.

[3] P. M. DeRusso, R. J. Roy, and C. M. Close, State Variables for Engineers. New York: John Wiley and Sons, Inc., 1965.

[4] J. R. Ragazzini and L. A. Zadeh, "The Analysis of Sampled-Data Systems," Trans. AIEE, vol. 71, Part II, pp. 225-234, November 1952.

[5] J. T. Tou, Digital and Sampled-data Control Systems. New York: McGraw-Hill Book Company, 1959.

[6] M. Athans, "The Role and Use of the Stochastic Linear-Quadratic-Gaussian Problem in Control System Design," IEEE Trans. Auto. Control, vol. AC-16, pp. 529-552, 1971.

[7] N. Halyo and A. Caglayan, "On the Discrete-Time Equivalent of the Stochastic Linear-Quadratic-Gaussian Sampled-Data Regulator Problem," submitted for publication.

[8] A. Peled and B. Liu, Digital Signal Processing. New York: John Wiley and Sons, Inc., 1976.

[9] J. S. Meditch, Stochastic Optimal Linear Estimation and Control. New York: McGraw-Hill Book Company, 1969.

[10] P. Dorato and A. Levis, "Optimal Linear Regulators: The Discrete-Time Case," IEEE Trans. Auto. Control, vol. AC-16, pp. 613-620, 1971.

[11] D. Luenberger, "An Introduction to Observers," IEEE Trans. Auto. Control, vol. AC-16, pp. 596-602, 1971.

[12] G. M. Kranc, "Input-Output Analysis of Multirate Feedback Systems," IRE Trans. Auto. Control, vol. AC-3, pp. 21-28, November 1957.

[13] W. H. Boykin and B. D. Frazier, "Analysis of Multiloop, Multirate Sampled-Data Systems," AIAA Journal, vol. 13, pp. 453-456, April 1975.

[14] E. I. Jury, "A Note on Multirate Sampled-Data Systems," IEEE Trans. Auto. Control (Corresp.), vol. AC-12, pp. 319-320, 1967.

[15] Ian B. Rhodes, "A Tutorial Introduction to Estimation and Filtering," IEEE Trans. Auto. Control, vol. AC-16, pp. 688-706, 1971.

[16] M. Sendaula, "Multidimensional State-Space Models for Linear Discrete-Time Multirate Systems," submitted for publication.

[17] W. Brogan, Modern Control Theory. New York: Quantum Publishers, Inc., 1974.